Joule

CellPress
REVIEWS

Review

Sr Segregation in Perovskite Oxides: Why It Happens and How It Exists

Bonjae Koo,[1,4] Kyeounghak Kim,[2,4] Jun Kyu Kim,[1,4] Hyunguk Kwon,[3] Jeong Woo Han,[2,*] and WooChul Jung[1,*]

Among the phenomena related to the surface rearrangement of cations in perovskite-based oxides, A-site cation enrichment, Sr in particular, near the surface has been frequently observed. Upon annealing in an oxidizing atmosphere, Sr is often enriched on the surface as compared with the bulk composition of the material, which eventually forms Sr-rich phases or rearranges the crystal structure of the surface. This Sr segregation changes the structure and composition of the perovskite surfaces and thus affects the stability of the materials and the reactivity with gas phases. In this regard, many studies have been carried out in the field of solid oxide electrochemical cells (SOCs). In this review, we summarize the latest research efforts on Sr segregation in perovskite-based SOC O_2 electrodes, with a focus on how excess Sr is present. We then discuss the origins of Sr segregation and suggest strategies for suppressing it to realize high-performance perovskite-based O_2 electrodes.

Introduction

Complex oxides composed of many different cations typically accommodate a range of stoichiometries and crystal structures, and thus exhibit a wide spectrum of properties according to changes in ionic radii, oxidation states, and coordination configurations of the constituent or dopant cations. Perovskite oxides with a chemical formula of ABO_3 are a representative example of this type of complex system. In the ABO_3 structure, "A" and "B" sites are occupied by two types of cations that are considerably different in size. The larger A-site cation, on the corners of the lattice, is usually an alkaline earth or rare-earth element, and the smaller B-site cation at the center of the lattice could be a 3d, 4d, or 5d transition metal element. A large number of metallic elements can thus be embedded in the perovskite structure. In addition, the ideal cubic crystal can be readily transformed to tetragonal, orthorhombic, and rhombohedral by slight distortion or buckling. Therefore, perovskite oxides are an important class of functional materials that can realize a variety of attractive properties, including ferroelectricity, piezoelectricity, dielectricity, ferromagnetism, magnetoresistance, multiferroics, superconductivity, and even catalysis, and are the basis for many existing electronic, electro-optical, electromechanical, and catalytic applications.[1–10]

Normally, in these complex oxides a loss of symmetry at the surface relative to the bulk induces a redistribution of cations, and therefore a specific cation accumulates selectively at oxide surfaces. This phenomenon, commonly referred to as cation segregation, notably alters the composition and structure of the oxide surface (or area near the surface), and this can have important (and often deleterious) effects on the overall surface properties of the materials. In particular, it has been frequently reported that the performance of electrodes or catalysts composed of perovskite oxides operating at high temperatures is strongly dependent on the cation

Context & Scale

Solid oxide electrochemical cells (SOCs) are a promising energy storage/conversion device that can store energy in the form of chemical fuels (electrolysis mode) or convert fuel to electricity (fuel-cell mode) with a remarkably high efficiency. A challenge to SOC development is the degradation of perovskite-based O_2 electrodes, primarily due to Sr segregation on the electrode surfaces at high operating temperatures. Despite many efforts, practical solutions have not yet been proposed to inhibit Sr segregation.

In this review, we classify recent discoveries of formations and structures of Sr segregation on perovskite surfaces, which allow us to clarify what Sr segregation is. We then reinterpret the research findings reported thus far to elucidate microscopic and macroscopic aspects of the segregation driving forces. The insights from this discussion present strategies to control Sr segregation and suggest new directions to be taken in the future to design the ideal O_2 electrode.

segregation.[11–32] A typical example is the surface chemical evolution of perovskite-based electrodes used in solid oxide electrochemical cells (SOCs), a next-generation energy conversion device. When perovskite oxides have been annealed in an oxidizing atmosphere, A-site cation segregation, Sr in particular, has frequently been observed on the surface, and Sr segregation has been suggested as a major reason behind the chemical instability of perovskite oxide surfaces and the corresponding performance degradation of SOC electrodes.[11–26] In recent years, to further improve device performance, research to identify the origins of this segregation phenomenon and to control the degree of cation enrichment has greatly advanced, and these tasks are among the central themes in current SOC electrode research.[33–38]

In this review, we summarize the latest research efforts to understand Sr segregation of perovskite-based electrode materials. Instead of presenting a comprehensive discussion of cation segregation at the perovskite oxide surface, which has already been summarized in earlier reviews,[39–41] we limit the topic to surface Sr excess in perovskite-based O_2-electrode materials for SOCs, and provide an in-depth discussion of the atomic level origins of this phenomenon. For this purpose, surface Sr segregation will clearly be defined, and its specific formations and structures observed so far will be clarified. We will also reinterpret the reported computational and experimental results, including our own findings, and extract the key driving forces that are common to them. Finally, based on this discussion and the insight it provides, we will present strategies to control the degree of Sr segregation and suggest new research directions that should be considered to achieve further ideal SOC O_2 electrodes.

Surface Cation Segregation in Perovskite Oxide

Since the surface of solid crystals is created by cleaving the bulk structure along a certain direction, surface atoms have lower coordination numbers than the bulk atoms. The exposed surface breaks the structural symmetry, which allows surface atoms generally to have different atomic arrangements compared with bulk atoms. This results in different levels of stability (e.g., free energy) between the surface and the bulk, and thus there exists a driving force to redistribute the surface atoms. With regard to perovskite oxides, because they contain many cations with different ionic characteristics, the surface redistribution typically involves some degree of enrichment or depletion of certain cations compared with the bulk composition. This segregation of constituent or dopant cations of the perovskite surface has been observed frequently and is known to have a strong influence on the surface composition and microstructure of the materials.

Let us consider briefly the processes of cation segregation (Figure 1A). First, the enrichment of particular cations will occur at the outermost surface while the original perovskite structure is maintained. In this case, atomic rearrangement may occur at the outermost surface by competition between different cations within the same site, or by competition between the A-site cation and the B-site cation: this latter situation is also described as surface termination. Then, when the cations accumulate to a level over the solubility limit, phase separation will take place. If the driving force of the segregation is large enough or the kinetic barrier of the phase separation is small enough, large clusters of the secondary phase can be created. Indeed, the extent of the segregation depends on the material composition and on the external conditions (i.e., temperature, oxygen partial pressure, electric field, etc.); typically, however, the segregation occurs more dynamically at higher temperatures, at which cations are more mobile in the crystal lattice and the rates of cation diffusion and

[1]Department of Materials Science and Engineering, Korea Advanced Institute of Science and Technology (KAIST), Daejeon 34141, Republic of Korea

[2]Department of Chemical Engineering, Pohang University of Science and Technology (POSTECH), Pohang 37673, Republic of Korea

[3]Department of Chemical Engineering, University of Seoul, Seoul 02504, Republic of Korea

[4]These authors contributed equally

*Correspondence: jwhan@postech.ac.kr (J.W.H.), wcjung@kaist.ac.kr (W.J.)

https://doi.org/10.1016/j.joule.2018.07.016

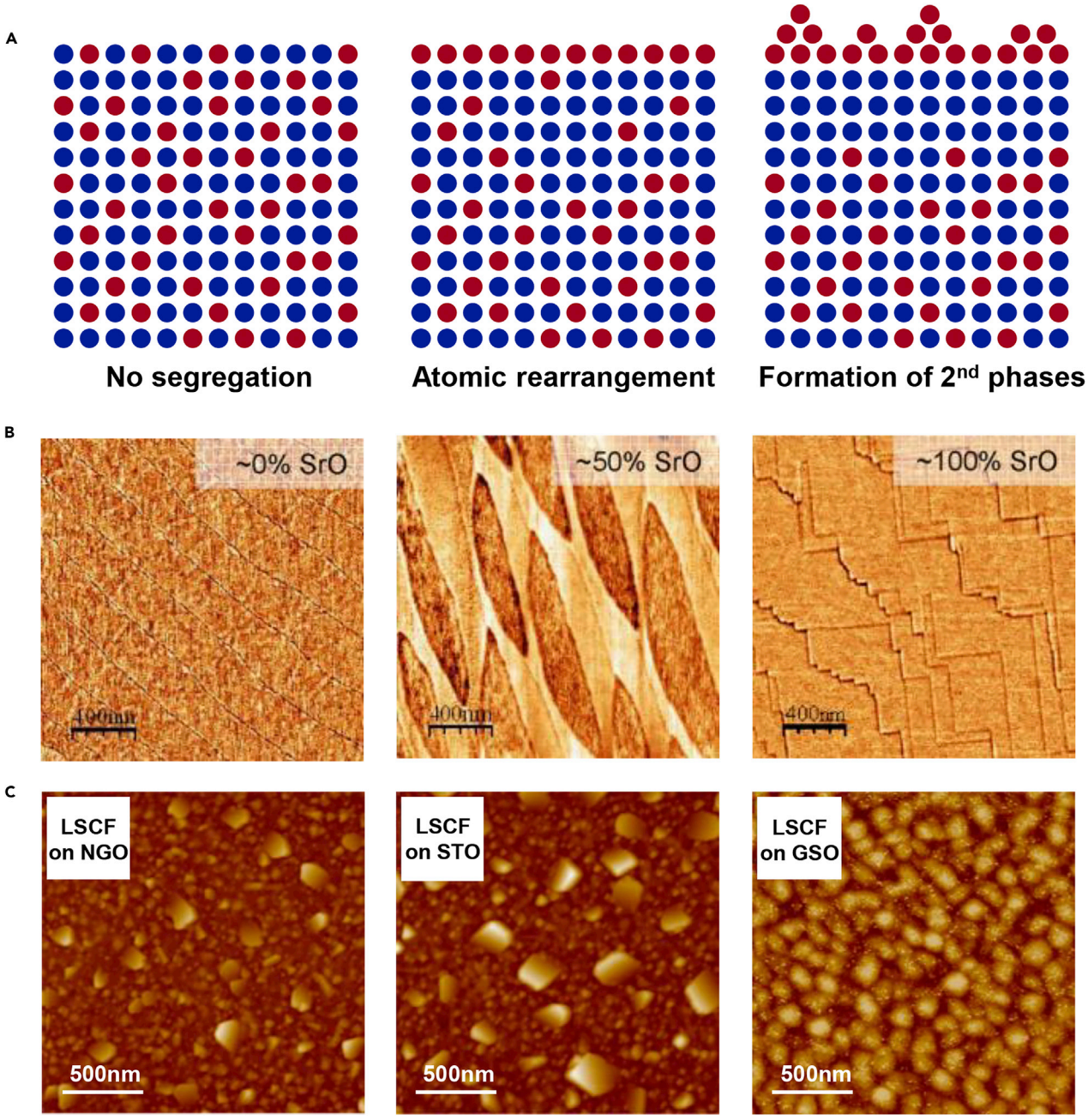

Figure 1. Surface Microstructure of Cation Segregation

(A) Schematic images of the surface cation segregation processes.

(B) The morphological and chemical evolution of the NH_4F buffered HF solution treated single-crystal (001)-$SrTiO_3$ substrate surface after annealing at 1,300°C for 2 hr, 12 hr, and 72 hr in air, respectively, by atomic force microscopy (AFM). Reprinted from Bachelet et al.,[42] with permission. Copyright 2009, American Institute of Physics Publishing.

(C) The surface topological images by AFM of annealed (001)-$La_{0.6}Sr_{0.4}Co_{0.2}Fe_{0.8}O_{3-\delta}$ (LSCF) thin films at 800°C for 10 hr in air on single-crystal (110)-$NdGaO_3$ (NGO), (001)-$SrTiO_3$ (STO), and (110)-$GdScO_3$ (GSO) substrate, respectively. The surfaces of each sample are covered by secondary-phase precipitates. Reprinted from Yu et al.,[36] with permission. Copyright 2016, American Chemical Society.

precipitate nucleation/growth are faster.[24–26,33–38,42–46] Good examples are found in reports on the surface evolution according to heat treatment of an $SrTiO_3$ single crystal with atomically flat surfaces. Bachelet et al. annealed a fully TiO_2-terminated

(001) $SrTiO_3$ single-crystal sample obtained via sophisticated chemical treatment at 1,300°C in air. As the annealing time increased from 2 hr to 12 hr and 72 hr, the ratio of SrO in the termination layer also increased from 0% to 50% and 100%, respectively (Figure 1B). They explained that this selective SrO termination was the result of thermally induced exdiffusion of Sr from the bulk.[42] On the other hand, SrO clusters on the surface of a single-crystal $SrTiO_3$ began to be observed when annealing proceeded at higher temperatures or when surface termination was not perfectly controlled with many defects.[43] Likewise, cation segregation phenomena have frequently been observed in materials used for devices operating at high temperatures. For the perovskite-based electrodes used for high-temperature fuel cells, electrolyzers for hydrogen production, and O_2 permeation membranes, specific A-site cations such as Sr^{2+}, Ba^{2+}, Pb^{2+}, and La^{3+} tend to segregate to the surface upon annealing.[11–38,44,46,47] Yu et al. investigated Sr-related precipitates on the surface of strain-controlled $La_{0.6}Sr_{0.4}Co_{0.2}Fe_{0.8}O_{3-\delta}$ epitaxial thin films after annealing at 800°C for 10 hr in air, as shown in Figure 1C.[36] Szot et al. observed Ba excess on the outermost surface of $BaTiO_3$ samples after these were annealed at 950°C for 5 hr in air.[47] Borca et al. also reported that precipitates of a Pb-rich phase formed on the surface of $La_{0.65}Pb_{0.35}MnO_{3-\delta}$ thin films after heat treatment at 520°C for several days.[31] This phenomenon, whereby the surface is enriched with a certain type of A-site cation, has been observed not only in a simple perovskite structure but also in derivatives of such a structure (e.g., double perovskite [$GdBaCo_2O_{5+\delta}$], Ruddlesden-Popper [$La_2NiO_{4+\delta}$], Aurivillius [Bi_2MoO_6 and Bi_2O_2 ($A_{n-1}B_nO_{3n+1}$)], among others).[30,48,49]

In addition to A-site cations, surface enrichment of B-site transition metals and subsequent phase separation have been reported. Upon high-temperature reduction, some transition metals dissolved in the lattice in an oxidizing atmosphere can be partially reduced and decomposed into nanosized metallic particles on the oxide surface. This *in situ* synthesis process of metal nanoparticles supported on an oxide host can be considered as one type of partial reduction/oxidation phenomenon of typical complex oxides[50] and is referred to as redox ex-solution. Compared with traditional nanoparticle synthesis and dispersion techniques, this process is faster and more cost-effective and allows finer and better particle distribution. More importantly, its reversibility indicates that the agglomeration of particles can be avoided through reoxidation, significantly enhancing the lifetime of the supported nanoparticles when they are used as a catalyst. Therefore, this process has attracted a great deal of attention recently in the fields of catalysis and renewable energy.[27,39–41] In summary, it is obvious that a variety of cations can be segregated on the surface of the perovskite oxide. Among them, however, the most widely known is surface Sr excess upon high-temperature oxidation, which is the subject of this review.

Effect of Sr Segregation on Perovskite Oxide Electrode for Solid Oxide Electrochemical Cells

As an environment-friendly future energy technology, SOCs have attracted considerable attention. SOCs are a general class of electrochemical devices using a solid oxide electrolyte, in which energy can be either stored in the form of a chemical fuel (electrolysis mode) or converted into electricity (fuel-cell mode). Typically, both modes of SOC operation exhibit remarkably higher efficiency compared with other related electrochemical devices. Moreover, they use an electrolyte that is an oxygen-ion conductor, providing much greater fuel flexibility than low-temperature devices based on proton-conducting electrolytes.[51–59] Thus, SOCs can operate in separate modes and also actively respond to dynamically changing energy demand and supply, especially in combination with renewable energy. However, a

long-standing bottleneck with regard to the commercialization of SOC technology is the high costs associated with cell fabrication and operation, largely attributed to the high operation temperature, which is typically in the range of 800°C–900°C. Over the past decade, considerable progress has been achieved in lowering this temperature (≤700°C), allowing us to reduce cost by using metallic interconnects and compressive nonglass/ceramic seals and to extend the lifespan by weakening chemical and mechanical degradation.[55] Nonetheless, the electrochemical resistance of an O_2 electrode increases rapidly at a lower temperature due to the high activation energy of the oxygen reduction/evolution reaction (ORR/OER). Thus, the development of high-performance O_2 electrodes has remained a tremendous challenge. For a comprehensive review of SOCs, please refer to other works in the literature.[39–41,51,53–59]

The key requirements for excellent O_2-electrode materials are as follows: they need to have high electronic and ionic conductivity, as well as favorable electrochemical reactivity toward ORR/OER. They also need to be stable for long duration in a high-temperature oxidizing atmosphere. In this respect, perovskite-based oxides can be good candidate electrodes, and many of the following compositions are actively used as SOC electrode materials: (La,Sr)(Co,Fe)$O_{3-\delta}$,[60–63] (La,Sr)(Mn,Fe)$O_{3-\delta}$,[13,64–66] (Ba,Sr)(Co,Fe)$O_{3-\delta}$,[5] Pr(Ba,Sr)(Co,Fe)$_2O_{5+\delta}$,[14] and Sr(Ti,Fe,Ni)$O_{3-\delta}$.[21,67] However, the chemical instability of their surfaces, particularly at elevated temperatures (>600°C), leads to severe degradation of the electrode performance over time. Surface cation segregation has recently been suggested as the key reason for the instability of perovskite-based electrode surfaces. Upon annealing in an oxidizing atmosphere, A-site cation segregation near the electrode surface has been widely reported. In particular, most electrode materials showing excellent initial performance contain Sr at the A site, and there are many reports that surface Sr segregation is closely related to the deterioration of SOC electrode performance.[11–26] For example, Cai et al. reported that the polarization resistance of the $La_{0.6}Sr_{0.4}CoO_{3-\delta}$ electrode increases by up to two orders of magnitude at 600°C within 72 hr, and correlated this with Sr segregation as shown in Figure 2A.[11] Pan et al. investigated the correlation between surface Sr segregation and performance in terms of time and temperature under open-circuit voltage conditions, suggesting that Sr segregation causes degradation of the $La_{0.6}Sr_{0.4}Co_{0.2}Fe_{0.8}O_{3-\delta}$ electrode.[15] Rupp et al. observed the deactivation of the $La_{0.6}Sr_{0.4}CoO_{3-\delta}$ thin-film electrode during the deposition of SrO in real time (Figure 2B).[18] Huber et al. reported that the deterioration of the surface activity of the $La_{0.8}Sr_{0.2}MnO_{3-\delta}$ electrode was due to changes in the surface composition caused by Sr segregation.[16] Jung and Tuller also observed a significant reduction in the polarization resistance of the $SrTi_{1-x}Fe_xO_{3-\delta}$ (x = 0.5 and 1.0) thin-film electrodes by chemically etching the Sr-enriched layer, and therefore confirmed that the segregated SrO_x serves as a passivation barrier for oxygen exchange (Figure 2C).[21] Most Sr-rich precipitates (e.g., SrO, $SrCO_3$, or $Sr(OH)_2$) produced as a result of severe Sr segregation are dielectrics. Thus, if they cover the perovskite surface, it is expected that electrochemically active sites will be passivated. However, in many cases the deterioration of the oxygen exchange rate and/or electrode polarization resistance of the Sr-segregated electrodes is much more severe (even sometimes more than a few orders of magnitude) than the surface coverage of the apparently observed Sr-excess clusters. Therefore, it should be emphasized that we cannot simply accept the direct correlation between the degree of surface Sr enrichment and the reactivity of the perovskite oxide surface. Despite some reports of surface Sr enrichment acting as a tunneling barrier for electron transfer or altering the electronic structure of the perovskite surface,[17,68] no consensus has yet been reached. Therefore, identifying the exact effect of Sr

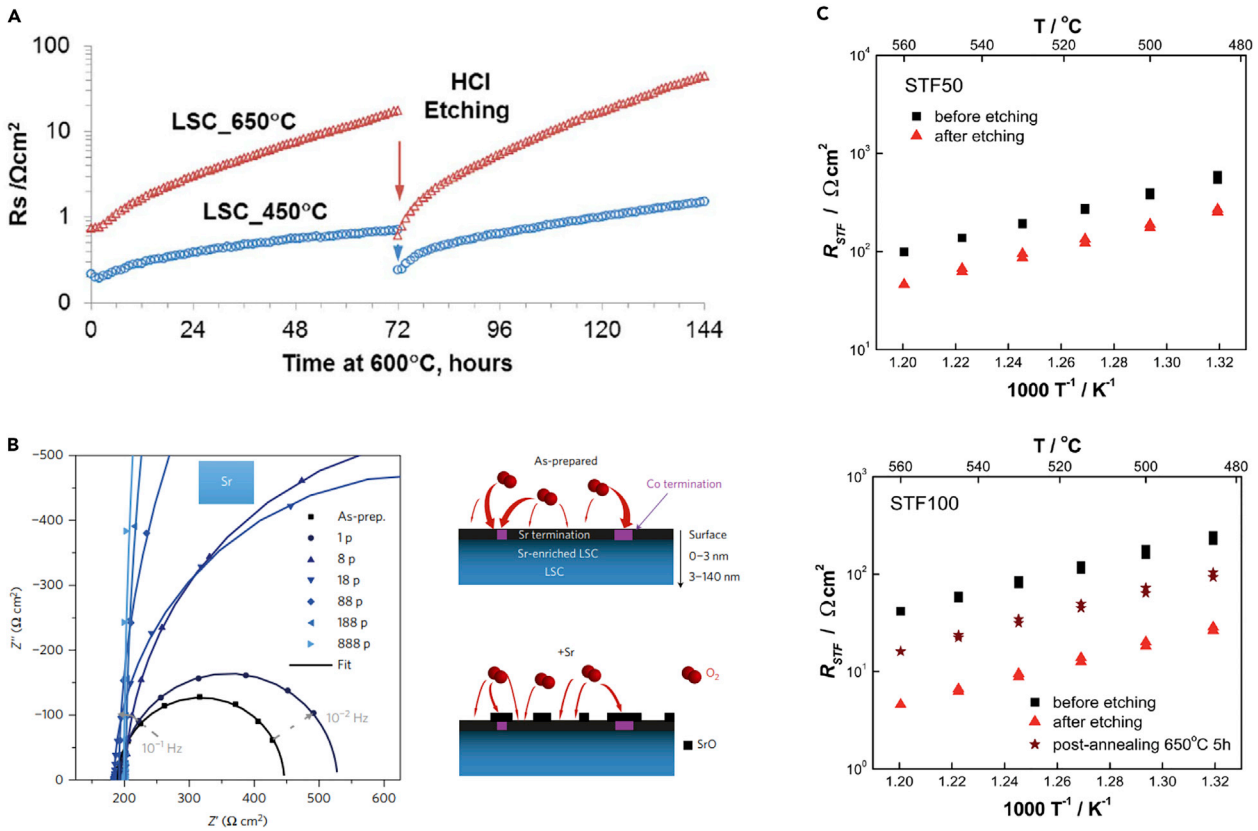

Figure 2. Correlation between Cation Segregation and Solid Oxide Electrochemical Cells Electrode Performance

(A) Surface polarization resistance, R_s, of $La_{0.6}Sr_{0.4}CoO_{3-\delta}$ films deposited by pulsed laser deposition (PLD) at 450°C (LSC_450°C) and 650°C (LSC_650°C). R_s was measured by impedance spectroscopy at 600°C in air before and after HCl etching. After etching, LSC_650°C degrades much faster than LSC_450°C, qualitatively similar to the case in the first 72 hr of annealing before etching. Reprinted from Cai et al.,[11] with permission. Copyright 2012, American Chemical Society.

(B) Evolution of the impedance spectra of the $La_{0.6}Sr_{0.4}CoO_{3-\delta}$ (LSC) thin-film electrode during the deposition of Sr. The impedance spectra were measured *in situ* at 450°C and $pO_2 = 5 \times 10^{-1}$ mbar. The legend shows the total number of laser pulses after which the impedance spectra were recorded (left). The authors assumed a process of decreasing surface activity by SrO coverage (right). Reprinted from Rupp et al.,[18] with permission. Copyright 2017, Springer Nature.

(C) Temperature-dependent surface polarization resistance, R_{STF}, of $SrTi_{1-x}Fe_xO_{3-\delta}$ (STF100x, x = 0.5 and 1.0) thin-film electrodes before (black square) and after (red triangle) etching, and after subsequent annealing at 650°C for 5 hr (brown star). Reprinted from Jung and Tuller,[21] with permission. Copyright 2012, Royal Society of Chemistry.

segregation on the inherent reactivity of the perovskite oxide surface is considered a key research topic in related fields. This requires techniques to precisely control and/or analyze the composition and structure of the outermost surface while evaluating the catalytic response of the oxide surface. A detailed analysis of the secondary-phase species on the surface and of the interface between the secondary phase and the host oxide is also required.

Surface Sr Segregation Phenomena

As mentioned above, this review focuses on the Sr segregation occurring on the surface of perovskite-based electrode materials at elevated temperatures. To establish a basis for understanding the origins of this segregation, we will first summarize the results observed so far in studies related to Sr segregation. In particular, we will discuss exactly what surface Sr segregation means and how a Sr-segregated layer is present.

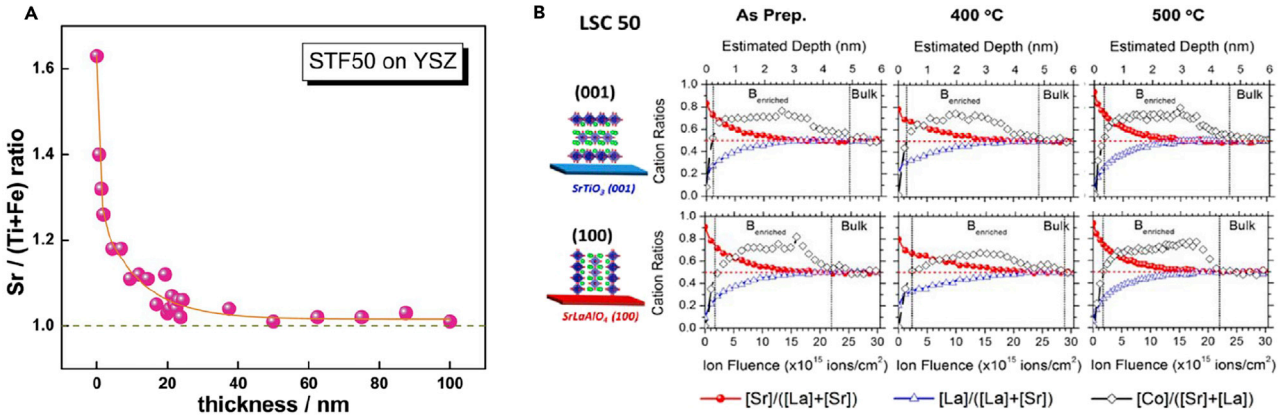

Figure 3. Depth Profile of Sr Segregation

(A) Depth-dependent chemical composition obtained for $SrTi_{0.5}Fe_{0.5}O_{3-\delta}$ (STF50) film on Y_2O_3-stabilized ZrO_2 (YSZ) by X-ray photoelectron spectroscopy (XPS). The amount of Sr with respect to the other component cations (Ti and Fe) decreases as a function of depth and nearly reaches the stoichiometry composition of perovskite. Reprinted from Jung and Tuller,[21] with permission. Copyright 2012, Royal Society of Chemistry.

(B) Depth-dependent chemical composition obtained for $(La_{0.5}Sr_{0.5})_2CoO_{4+\delta}$ (LSC50) films with (001) orientation (top) and (100) orientation (bottom) by low-energy ion scattering. The depth profiles demonstrate the surface and near-surface restructuring by Sr segregation of as-prepared and heat-treated samples. The heat treatment was done at 400°C and 500°C, respectively for 10.25 hr. Reprinted from Chen et al.,[24] with permission. Copyright 2015, American Chemical Society.

Terminology Definition

Before looking at it in detail, we need to clearly define the term "segregation." In fact, "segregation" is a word that refers to the enrichment of atoms, ions, or molecules at a microscopic region in a materials system and is often assigned slightly different meanings in various fields. However, "equilibrium segregation," depicted in earlier classical theories (i.e., Gibbs Adsorption Isotherm or Langmuir-McLean Isotherm), refers only to the partitioning of a solute or defect to a surface or grain boundary in a single phase.[69] In this case, if the addition of a solute or defect to a system lowers the surface energy of the oxide/gas interface, the species will segregate preferentially toward the surface. Thus, the surface we referred to here is a Gibbs' ideal model interface, and in this case the segregation represents a solute excess only at the outermost surface.

On the other hand, the expression "Sr segregation," which is mainly referred to in high-temperature electrochemical applications, often involves an appreciable degree of Sr excess and the resulting formation of secondary phases near the perovskite-related oxide surface.[11–26,33–38,42–45,70–84] For example, Jung and Tuller reported that the depth of a heavily Sr-enriched region in $SrTi_{1-x}Fe_xO_{3-\delta}$ (x = 0.5 and 1.0) thin-film samples extends to about 10 nm from the surface, as shown in Figure 3A.[21] Szot et al. also observed that the outermost surface of $SrTiO_3$ was reconstructed to form SrO-rich phases.[70,71] Lee et al. observed SrO islands appearing on the surface when Sr-doped $LaMnO_3$ thin film was heat treated.[35] Niania et al. reported that Sr-containing compounds precipitated as a result of decomposition at the $La_{0.6}Sr_{0.4}Co_{0.2}Fe_{0.8}O_{3-\delta}$ surface.[44] Similarly, Chen et al. verified by low-energy ion scattering (LEIS) analysis that the area showing the inhomogeneity of the composition of a $(La_{0.5}Sr_{0.5})_2CoO_{4+\delta}$ thin film has a depth of about 5 nm from the surface (Figure 3B).[24] These observations extend beyond the selective segregation of a solute on the outermost surface defined in the classical theories. Therefore, the term "Sr segregation" used in this review broadly refers to the phenomenon of considerable Sr accumulation near the surface, and the term will be used synonymously with terms such as "Sr excess" and "Sr enrichment."

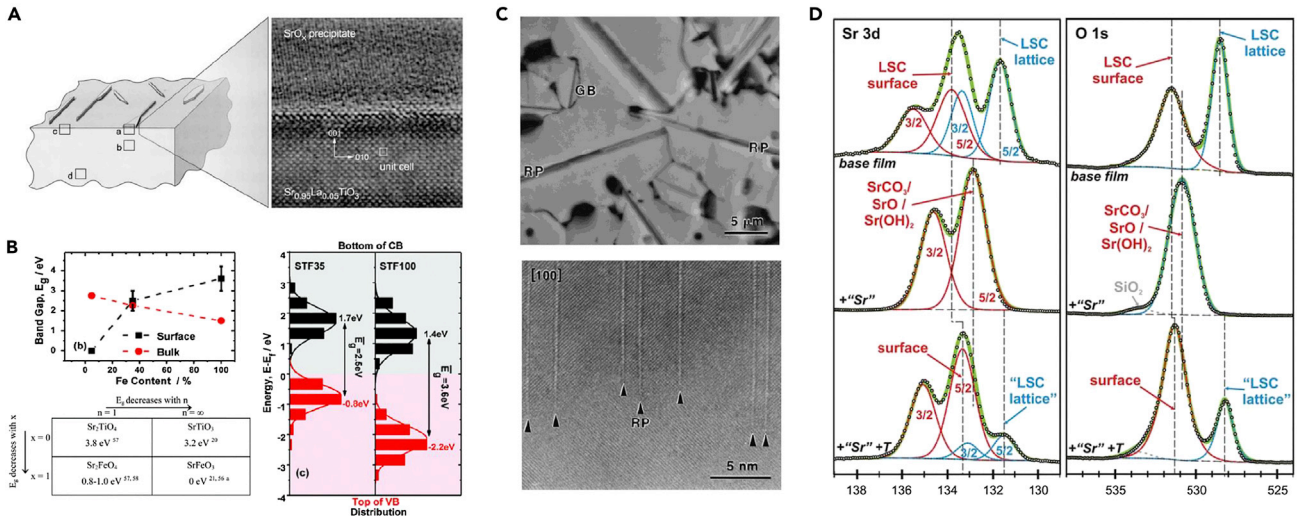

Figure 4. Various Formations and Structures of the Sr-Segregated Layer

(A) High-resolution transmission electron microscopy (HRTEM) image of the interface between (100)-oriented $Sr_{0.95}La_{0.05}TiO_3$ single crystal and a SrO precipitation. Reprinted from Meyer et al.,[74] with permission. Copyright 2002, Springer Nature.

(B) Comparison of the band gap (left) and band edges (right) at the surface measured by scanning tunneling spectroscopy (STS) for $SrTi_{1-x}Fe_xO_{3-\delta}$ (x = 0.35 and 1.0) thin films as a function of Fe content. STS analysis confirms that the segregated Sr phase exists in the form of SrO_x. The STS was measured at 345°C and $pO_2 = 1 \times 10^{-3}$ mbar. Reprinted from Chen et al.,[17] with permission. Copyright 2012, Royal Society of Chemistry.

(C) HRTEM images of the interface between the perovskite matrix and a Ruddlesden-Popper (RP) region in SrO-doped $SrTiO_3$. GB, grain boundary. The arrows indicate RP region. Reprinted from Šturm et al.,[88] with permission. Copyright 2000, Materials Research Society.

(D) X-ray photoelectron spectroscopy (XPS) results of base $La_{0.8}Sr_{0.2}CoO_{3-\delta}$ film, after Sr decoration with 1,000 laser pulses by pulsed laser deposition, and after heat treatment at 510°C for 4 hr at pO_2 = 1 atm. Reprinted from Mutoro et al.,[23] with permission. Copyright 2011, Royal Society of Chemistry.

Moreover, we will consider not only the surface rearrangement of the Sr cation as an aliovalent dopant with an effectively negative (or positive) charge (i.e., $La_{1-x}Sr_xCoO_{3-\delta}$ and $La_{1-x}Sr_xMnO_{3-\delta}$), but also the case in which Sr is the neutral constituent in the perovskite structure (i.e., $SrTiO_3$). The dopant segregation and the surface enrichment of the host cation are not precisely the same phenomenon. However, the perovskite materials used in most high-temperature electrochemical applications, especially materials with high Sr segregation, already contain significant amounts of Sr at the A site within the lattice. In fact, these are in the form of Sr-included solid solutions, where Sr is one of the main constituents determining the structural and chemical properties and electronic structures of the material and thus cannot be regarded as a dilute dopant in a strict sense. Therefore, we will discuss the phenomenon of Sr excess on the perovskite surface at high temperatures, regardless of whether Sr is the dopant or the main constituent.

Formation and Structure of the Segregated Sr Layer

To understand the nature of the Sr excess at the surface, we need to clarify its form. In principle, Sr can segregate as oxides (SrO_x), reconstructed Sr-excess phases ($SrO \cdot n(ABO_3)$), and/or reaction products formed with chemisorbed gases ($SrCO_3$ or $Sr(OH)_2 \cdot H_2O$) (Figure 4). Many surface analyses such as photoelectron spectroscopy, ion scattering, electron diffraction, and microscopy have revealed the detailed formation of segregated Sr layers in perovskite oxides, including $SrTiO_3$, $Sr(Ti,Fe)O_{3-\delta}$, $(Sm,Sr)CoO_{3-\delta}$, $(La,Sr)MnO_{3-\delta}$, $(La,Sr)CoO_{3-\delta}$, $(La,Sr)(Co,Fe)O_{3-\delta}$, and so on.[11–26,33–38,42–45,70–84]

Excess Sr in the form of an oxide has commonly been observed on the surface of perovskite materials, and three different species have been reported in this

case: SrO island precipitation, a reconstructed Sr-excess phase ($SrO \cdot n(ABO_3)$), and SrO excess in a cubic perovskite phase (ABO_3). The formation of SrO precipitates is the most widely reported instance of Sr segregation in perovskite oxides.[11–13,15–25,28,35,37,42,43,70,71,73–75,82] Szot et al. combined secondary ion mass spectroscopy (SIMS), atomic force microscopy (AFM), and X-ray photoelectron spectroscopy (XPS) to reveal that when a single-crystal $SrTiO_3$ is annealed at high temperatures for a long period of time, SrO_x accumulates in the form of a liquid phase on the surface and then recrystallizes to SrO.[43,70,71] Meyer et al. observed the formation of SrO clusters on the surface of La-doped $SrTiO_3$ by high-resolution transmission electron microscopy (HRTEM) (Figure 4A).[74] By analyzing depth and take-off angle-dependent XPS spectra, in combination with chemical and thermal treatments, Jung and Tuller suggested that surface Sr excess in $SrTi_{1-x}Fe_xO_{3-\delta}$ (x = 0.5 and 1.0) is largely accommodated by the formation of an Sr-excess phase ($SrO \cdot n(ABO_3)$) or SrO island precipitate.[21] In a subsequent study using $SrTi_{1-x}Fe_xO_{3-\delta}$ (x = 0.05, 0.35, and 1.0), Chen et al. analyzed the change of the surface band structure according to Fe concentration by *in situ* scanning tunneling microscopy/spectroscopy (STM/STS), and clarified that the Sr segregation layer is more likely to be in the form of SrO_x, as shown in Figure 4B.[17]

Except for island formation, other structures of excess Sr require a certain solubility of SrO in the perovskite lattice. Both experimental and theoretical analyses demonstrate that the cubic perovskite structure can accommodate only limited amounts of excess SrO in the form of solid solution, i.e., less than 0.2 mol% SrO in $SrTiO_3$.[85] Thus, a considerable amount of Sr accumulation cannot be explained simply by the change in Sr non-stoichiometry or SrO surface termination in a perovskite lattice, but always involves surface phase separation. Likewise, many researchers suggested that the incorporation of planar defects in the form of rock salt structured layers is the likely mechanism for the accommodation of SrO excess.[71,72,86–88] These planar defects are the additional SrO interlayers in a bulk lattice, which form a structurally reconstructed Sr-excess phase ($SrO \cdot n(ABO_3)$), often referred to as the Ruddlesden-Popper (RP) phase.[86–88] Indeed, RP phases have been found not only in SrO-excess ABO_3 systems, but also in stoichiometric ABO_3, where the A sites are partially or fully occupied by Sr atoms, including $(La,Sr)MnO_{3-\delta}$ and $SrTiO_3$. For example, Šturm et al. observed RP phase penetrating grain boundary between $SrTiO_3$ grains in SrO-excess $SrTiO_3$ sintered in air at 1,450°C for 10 hr, as shown in Figure 4C.[88] Dulli et al. found that the Sr segregation in $La_{0.65}Sr_{0.35}MnO_{3-\delta}$ caused a major restructuring of the surface region to form an RP phase $(La,Sr)_{n+1}Mn_nO_{3n+1}$ with n = 1.[72] Szot et al. found the growth of steps perpendicular to the surface with a height larger than the unit cell of the perovskite structure on the surface of oxygen-annealed $SrTiO_3$. In particular, crystals prepared above 900°C exhibited a step height of 11.8 Å, which is attributed to the formation of an RP phase ($SrO \cdot n(SrTiO_3)$) with n = 1 on the surface.[71]

Lastly, there are also cases in which Sr compounds are observed on the surface as reactants with CO_2 or H_2O in air.[11,22–25] Mutoro et al. reported through XPS analysis that most of the particles formed on the surface of $La_{0.8}Sr_{0.2}CoO_{3-\delta}$ thin film consisted of $SrCO_3$, which decomposed upon annealing at 510°C for 4 hr at pO_2 = 1 atm (Figure 4D).[23] Cai et al. suggested that most of the Sr-related compounds on the surface of $La_{0.6}Sr_{0.4}CoO_{3-\delta}$ thin film originate in the formation of $Sr(OH)_2$ from separated SrO phase.[11]

Based on the discussion thus far, the phenomenon we call "Sr segregation" can have different formations and structures depending on the compositions of the perovskite oxide, the synthesis processes, and the measurement conditions. It can also be seen

that the degree of Sr excess and the depth of the Sr-enriched region vary greatly depending on the given situation. Therefore, for the study of Sr segregation in-depth analysis of Sr-rich regions (and also nearby Sr-depleted regions) should first be carried out with a high level of precision.

Driving Forces of Sr Segregation

Selective accumulation of impurities or alloying elements at grain boundaries (GBs) of metallic alloys leads to the fracture of the grain boundary as a result of temper brittleness, creep embrittlement, or GB corrosion. Thus, GB segregation has been studied for a long time in the field of metallurgy. The driving force of the atomic movement in GB is very similar to that of surface segregation, which can be interpreted in terms of atomic arrangements different from the bulk, and the analytical equation can be derived in a similar form. Therefore, we will first briefly review the development of theoretical analysis of segregation phenomena near the GB. We will then expand this review to an analysis of the surface segregation behavior.

For the theoretical interpretation of GB segregation phenomena, McLean proposed the relationship between the mole fractions at GB and in the bulk and the free energy of segregation (ΔG_{seg}), as

$$\frac{X_g}{X_g^o - X_g} = \frac{X_b}{1 - X_b} \exp\left(-\Delta G_{seg}/kT\right),$$

where X_g and X_b are the solute mole fractions at the GB and in the bulk, respectively, X_g^o is the saturation value for X_g, ΔG_{seg} is the free energy of segregation, k is Boltzmann's constant, and T is absolute temperature.[69] To treat ΔG_{seg}, Tran et al. introduced the elastic strain energy of ΔE_{ela}, developed by Friedel:[89,90]

$$E_{ela} = \frac{24\pi K G r_1 r_2 (r_1 - r_2)^2}{4G r_1 + 3K r_2},$$

where K is the bulk modulus of the solute, G is the shear modulus of the solvent, and r_1 and r_2 are the effective radius of the solvent and the solute atoms, respectively. However, significant disagreement was observed at Σ5(310) Mo GBs between the density functional theory (DFT)-calculated and the McLean model-based dopant segregation energies.[90] Since the McLean model did not consider the electronic structure of metal alloy, it might have a limitation at predicting the segregation tendency of the dopant elements in metal alloys. In this regard, Mukherjee and Morán-López predicted the segregation tendency of 702 transition metal alloys through their internal electronic energies calculated from the bandwidth, band center, and fractional band filling of transition metals.[91] Despite the lack of consideration of elastic contribution, most of the predicted results showed reasonably good agreement with the experimental results, implying that electronic interaction is more critical than elastic contribution in predicting dopant segregation in metal alloy systems.

Considering both the elastic (Friedel model) and electronic (chemical bond strength) contributions, Wynblatt and Ku[92] and Desu and Payne[93] extensively described the free energy of segregation in alloy metals (ΔG_{seg_metal}) using three important factors: (1) interfacial energy, ΔG_{int}, (2) binary interaction between host and dopant metals, ΔG_{bin}, and (3) strain energy, ΔG_s (E_{ela}), i.e.,

$$\Delta G_{seg\_metal} = \Delta G_{int} + \Delta G_{bin} + \Delta G_s.$$

Significantly, this equation showed good agreement with the experimental results.[94] Løvvik showed linear relationships of DFT-calculated segregation energy of

Pb-based alloy metals, with the metal radius of the substituted atoms and the experimental surface energy as the indicators of elastic and electronic effects on the metal segregation, respectively.[95] Han et al. also predicted the segregation energies of all combinations of 3d, 4d, and 5d metals on flat, stepped, and kink surfaces in terms of coordination number, bond strength, and d-band center.[96]

However, such an analysis cannot directly be extended to the oxide materials. One major difference between metals and metal oxides is in the charge states; these do not exist in the metal alloys, which are uncharged mixed metals. For example, oxides contain negatively charged oxygen ions, which easily transform to the gas phase according to the working environments and change the oxidation state of cations accordingly. In addition, in oxides the formation of various types of defects (Schottky or Frenkel defects) and the transport of oxide ions or cations also often occur. In particular, the co-existence of cations and anions creates electrostatic interactions. These unique characteristics of oxide materials, including perovskites, do not exist in metals.

Elastic Contribution to Sr Segregation

In perovskite structures, A-site cations have a coordination number of 12 in the defect-free state. Once other kinds of cations are doped at the A site, the size mismatch between dopant and host cations causes elastic energy. To minimize this elastic energy within the materials, cation rearrangement might occur, which results in cation segregation. This leads to some degree of enrichment and depletion of cations at the surface and in the bulk, respectively. Thus, the segregation behavior is first associated with the elastic energy contribution. This elastic energy is commonly generated by the size mismatch at the A site between the host (La) and dopant (Sr), which can be controlled by doping of the A-site and B-site cations, and/or the lattice strain in (La,Sr)BO_3-type perovskites.[33–36,38,97] To identify the contribution of elastic energy induced by cation size mismatch at the A site, Lee et al. compared the DFT-calculated segregation energies and the elastic energies analytically calculated from the Friedel model in A-site doped $LaMnO_3$ and $SmMnO_3$.[35] They used Ca, Sr, and Ba, with charges of +2, as dopant cations in order to systematically cause elastic energies, and showed that a larger dopant tends to segregate more strongly toward the surface due to the greater amount of elastic energy generated in the system. This result indicates that the elastic energy induced by size mismatch between Sr and other cations present at the A site can significantly drive Sr segregation as shown in Figure 5A. Likewise, the thermodynamic tendency of Sr segregation toward the surfaces was also observed in $La_{0.7}Sr_{0.3}MnO_{3-\delta}$ and $La_{0.8}Sr_{0.2}CoO_{3-\delta}$ perovskite oxides in other DFT studies.[33,34,38,97,98]

Based on this understanding, it was reasonably expected that doping of Ca, which is smaller than Sr, at the A site of (La,Sr)CoO_3 may inhibit surface segregation, and thus improve electrochemical stability by reducing elastic interactions. To prove this, Koo et al. first developed a theoretical model based on the fractional free volume, which is defined as the free volume of an A-site doped perovskite oxide normalized by the unit cell volume. A combination of DFT calculations and corresponding experiments then demonstrated that electrochemical degradation induced by the segregation can be reduced considerably by Ca doping.[38] These experiments confirmed that the A-site dopant segregation was suppressed by increasing the fractional free volume in the perovskite oxides. In a similar way, Yoo et al. were also motivated to enhance the stability of perovskite oxide through A-site doping. Just by substituting Ca into the A site of $NdBaCo_2O_{5+\delta}$, they designed a perovskite oxide, $NdBa_{0.75}Ca_{0.25}Co_2O_{5+\delta}$, with improved electrochemical

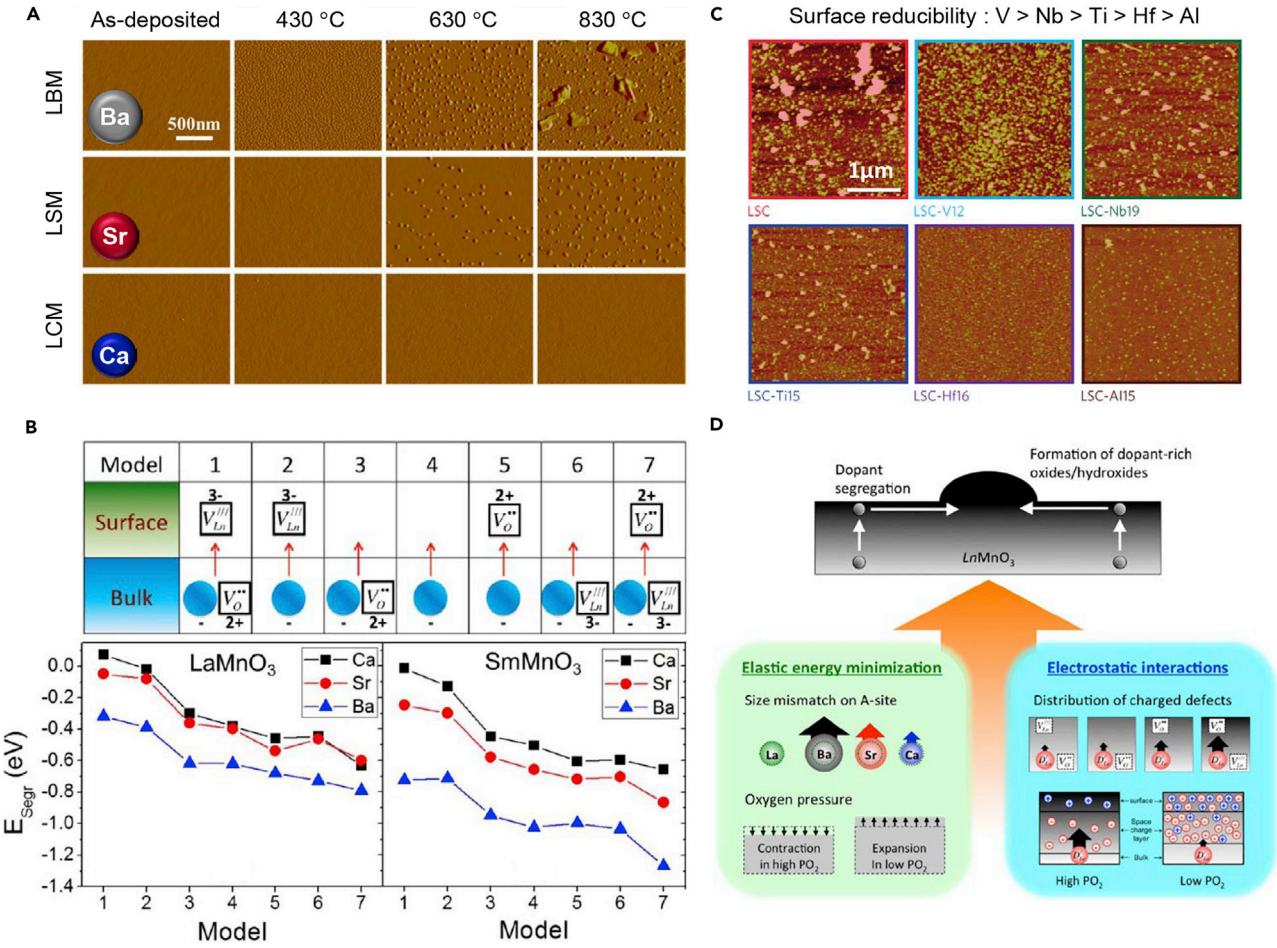

Figure 5. Atomic-Scale Factors Controlling Sr Segregation

(A) Surface morphology images of the Ba-, Sr-, and Ca-doped $LaMnO_3$ thin films (LBM, LSM, and LCM, respectively) as a function of annealing temperature (as-deposited, 430°C, 630°C, and 830°C, respectively) by atomic force microscopy (AFM).

(B) Seven models to represent different electrostatic interaction that are induced by controlling the distribution of charged oxygen and cation vacancies (top). Surface segregation energies of Ca, Sr, and Ba dopant on $LaMnO_3$ and $SmMnO_3$ surfaces obtained by density functional theory calculation within different electrostatic interaction models (bottom).

(C) Surface morphology images of the $La_{0.8}Sr_{0.2}CoO_{3-\delta}$ (LSC), 12 at% V-doped LSC (LSC-V12), 19 at% Nb-doped LSC (LSC-Nb19), 15 at% Ti-doped LSC (LSC-Ti15), 16 at% Hf-doped LSC (LSC-Hf16), and 15 at% Al-doped LSC (LSC-Al15) films after impedance spectroscopy test at 530°C in air by AFM. Reprinted from Tsvetkov et al.,[106] with permission. Copyright 2016, Springer Nature.

(D) Illustration of the mechanisms that drive dopant segregation to the surface of $LnMnO_3$ (Ln = Lanthanide). The schematic shows the two kinds of energy; elastic energy and electrostatic energy.

(A), (B), and (D) were reprinted from Lee et al.,[35] with permission. Copyright 2013, American Chemical Society.

performance and long-term stability under air and CO_2-containing atmosphere.[99] In addition, the effect of B-site cations on Sr segregation was reported based on the first-principle calculations by Kwon et al.[97] They used first-row 3d-transition metals as B-site cations ($Cr_{0.50}Mn_{0.50}$, Mn, Fe, $Co_{0.25}Fe_{0.75}$, Co, and Ni) to systemically generate the elastic energy in $(La,Sr)BO_3$ perovskites. Their results showed that choosing a smaller B-site cation, such as Co or Ni, thermodynamically weakens the elastic energy in the system and thus can suppress the segregation of Sr dopant.

The formation of A-site defects can also control the elastic energy by generating free space in materials, thereby influencing the cation segregation.[100] Jin and Lu found that as the A-site cation is deficient from a stoichiometric composition, the surface

Sr and La enrichment decreased after annealing at 500°C for 5 hr for $(La_{0.8}Sr_{0.2})_xMnO_{3-\delta}$ (x = 0.95–1.05).[101] Lee et al. also reported that A-site deficient $(La_{0.8}Sr_{0.2})_{1-x}MnO_{3-\delta}$ (x > 0) films show higher chemical stability against Sr segregation upon thermal annealing, whereas over-stoichiometry (x < 0) facilitates segregation. Since an A-site deficient film can accommodate more Sr cations in the lattice than can the ideal $La_{0.8}Sr_{0.2}MnO_{3-\delta}$ film, Sr dopant in the A-site deficient film can be stabilized despite compressive microstrain applied to the neighboring atoms by the Sr dopant, which is larger than the La host. The larger amount of space available in the lattice for rearranged cations upon annealing results in the higher stability of the A-site deficient $La_{0.8}Sr_{0.2}MnO_{3-\delta}$ films against the formation of secondary phase at the surface.[26] Since the cation defects can also change the free space in the perovskite structure, the fractional free volume suggested above might be effectively used as a descriptor to predict the degree of electrochemical stability.

Interestingly, the elastic contribution to Sr segregation discussed so far can also be applied to other perovskite systems, in which Sr is a main constituent, like $SrBO_3$. Since the stability of $SrBO_3$ is an outcome of the combined stabilities of the Sr-O and B-O bonds within the lattice, the perovskite structure reaches the most stable state when the two bonds are "properly" balanced. This, in turn, means that Sr atoms may not always be at the most stable state but are intrinsically unstable, even though the overall $SrBO_3$ perovskite structure is stable. Very recently, Koo et al. demonstrated that the degree of Sr enrichment at the surface of $SrTi_{0.5}Fe_{0.5}O_{3-\delta}$ epitaxial thin films can be controlled through lattice strain.[37] The tensile strain in the in-plane direction considerably inhibits Sr enrichment and also facilitates the surface O_2 exchange rate. This observation cannot be interpreted simply by the fractional free volume because the unit cell volume of $SrTi_{0.5}Fe_{0.5}O_{3-\delta}$ also increased as a function of tensile strain with the increase of the free volume. Instead, DFT calculations revealed that in unstrained $SrTiO_3$ perovskite, the large Sr atom is under a local compressive state, whereas the small Ti atom is under a local tensile state. Thus, although neither the Sr-O nor the Ti-O bonds may be in the most stable state individually, they are in an optimal balance at zero strain, thereby stabilizing the overall perovskite. Based on these observations, Koo et al. proposed that the extent of deviation from the optimal A-O bond strength in the most stable state of the A-site cation can be a driving force for surface segregation in ABO_3-type perovskite oxides. To confirm this hypothesis, they also attempted to expand the bond length (to fortify the bond strength) of Sr-O by doping with Hf or Zr, which is larger than Ti at the B site; this isovalent doping successfully suppressed the surface Sr excess in $SrTi_{0.5}Fe_{0.5}O_{3-\delta}$.[37] Similarly, Jung and Tuller reported that a greater extent of Fe in Ti increases the degree of Sr segregation because the ionic radius of Fe is lower than that of Ti.[21]

For (La,Sr)BO_3-type perovskites, lattice strain can also be an effective way to control elastic interactions. Based on a combined theoretical and experimental analysis, Yildiz's group showed that Sr segregation increases as the in-plane lattice strain increases from compressive to tensile state in $La_{0.7}Sr_{0.3}MnO_{3-\delta}$ and $La_{0.8}Sr_{0.2}CoO_{3-\delta}$ perovskites.[33,34] Based on the DFT calculations, Ding et al. also reported that external tensile strain reinforces the thermodynamic tendency of Sr surface segregation in $La_{1-x}Sr_xCo_{1-y}Fe_yO_{3-\delta}$ perovskite.[102] Unlike $SrTiO_3$-like materials, however, in this type of material, the strain response to Sr segregation seems to be the opposite: lattice strain enhances Sr segregation. This may be attributed to the different response of the Sr-O bond strength to the applied strain between the two types of materials. This idea should be more intensively investigated in the future.

Electrostatic Contribution to Sr Segregation

The surfaces of solids are inherently charged, at minimum due to the preferential adsorption of selected gas-phase species. In an ionic solid, the loss of symmetry at the surface relative to the bulk additionally induces a redistribution of anions and cations, which becomes another source of surface charge. This surface charge can be the electrostatic driving force for Sr segregation. Typically, the perovskite oxides used in SOC O_2 electrodes readily form oxygen vacancies, which may accumulate more on the surface that has lower coordination compared with the bulk. These excessive oxygen vacancies have been suggested to make the oxide surface to be positively charged, and thus induce the cation segregation.[103–105] For example, Sr substituted with La^{3+} in $LaBO_3$ perovskite (Sr'_{La} in Kröger-Vink notation) has an effective charge of −1 relative to the original crystal lattice. This implies that the negatively charged Sr can be attracted according to Coulomb's law by the positively charged surface oxygen vacancies.[35] The DFT results from Lee et al. showed that O vacancy of +2 charge at the surface and La vacancy of −3 charge in the bulk strengthen the thermodynamic tendency of Sr atoms to segregate toward the surface by both electrostatic attraction toward the surface and repulsion from the bulk, as shown in Figure 5B.[35] Ding et al. theoretically demonstrated that the surface charge can be tuned by doping with different valence elements at A or B sites in $La_{1-x}Sr_xCo_{1-y}Fe_yO_{3-\delta}$, where increasing the surface charge enhances the Sr segregation.[102] In this sense, Tsvetkov et al. showed surface modification of $La_{0.8}Sr_{0.2}CoO_{3-\delta}$ perovskite with less-reducible B-site cations than Co, such as Hf^{4+}, Ti^{4+}, Zr^{4+}, Nb^{5+}, or Al^{3+}, to decrease the oxygen vacancy concentration at the surface. Their experimental results proved that Sr enrichment decreases with the addition of more reducible cations, especially Hf^{4+} or Zr^{4+}, due to the reduction of electrostatic attraction to Sr atom from the surface (Figure 5C).[106]

The quantity of surface oxygen defects is affected by the chemical potential of oxygen gas at equilibrium with the oxide. Thus, investigating the segregation tendency with regard to the oxygen partial pressure may be a way to explore the relationship between surface oxygen vacancy and cation segregation. Fister et al. used experimental measurements to calculate the enthalpy of Sr as a function of the oxygen partial pressure in the range of pO_2 = 1.5–150 Torr in $La_{0.7}Sr_{0.3}MnO_{3-\delta}$. They showed that Sr segregation toward the surface is thermodynamically preferred over all pO_2 conditions. It was also found that segregation is enhanced with decreasing pO_2 due to the electrostatic interaction between the charged point defects of oxygen vacancies and Sr dopants.[107]

It is noteworthy that the nature of polar surfaces in perovskites needs to be considered to understand the segregation behavior in the aspect of electrostatic interaction. The typical perovskites of ABO_3 commonly consist of AO and BO_2 planes with -$(AO\text{-}BO_2)_n$-stacking sequences. The A and B cations in a perovskite such as $SrTiO_3$ have charges of 2+ and 4+, respectively, which makes both $A^{2+}O^{2-}$[0] and $B^{4+}O_2{}^{2-}$[0] planes formally neutral. In this case, the contribution of elastic interaction may be significant. On the other hand, if A and B cations both have charges of 3+ such as $LaMnO_3$, the AO and BO_2 planes have formally positive and negative charges ($A^{3+}O^{2-}$[+1] and $B^{3+}O_2{}^{2-}$[−1]), respectively, giving the perovskites an alternatively charged stack and causing the surfaces to be polar. For perovskites in which the A and B cations have charges of +1 and +5, respectively such as $KTaO_3$, this is similar, but with oppositely charged sequences ($A^{1+}O^{2-}$[−1] and $B^{5+}O_2{}^{2-}$[+1]). In this sense, replacing the surface with differently charged cations can be a way to neutralize the charged surface and thus suppress cation segregation. Ding et al. suggested that the lower surface charge of the SrO-terminated surface (+0.52e) relative

to that of the LaO-terminated surface (+1.35e) may drive Sr segregation toward the surface of $La_{1-x}Sr_xCo_{1-y}Fe_yO_{3-\delta}$.[102] In other words, if the surface charge can be reduced by forming a SrO-terminated surface with segregated Sr, the surface would be stabilized due to the lowered surface energy. Druce et al. also reported that because typical perovskites used as SOFC cathodes often have a charge of 3+ for both the A and B cations, the Sr^{2+} dopant would segregate to the outer surface to decrease the surface energy by neutralizing the charged surface.[30] Harrison theoretically discussed how the neutralization of the surface charge, which may be one of the reasons for Sr segregation at (La,Sr)MnO_3, can be obtained by either changing the Mn charge states or readjusting the molar ratio of La/Sr on the surface plane, both of which modify the elastic and electrostatic energies simultaneously.[111]

Until now, most research has analyzed the elastic and electrostatic contributions to Sr segregation separately, as introduced earlier in this section. Strictly speaking, however, it is difficult to completely decouple the two contributions from each other. For example, doping of a B-site cation has a considerable effect on the elastic interaction by changing the unit cell volume. Simultaneously, it can also change the concentration of oxygen vacancies due to the change of reducibility, thereby affecting the electrostatic interaction. As mentioned above, Kwon et al. demonstrated that the addition of a smaller B-site cation (Co or Ni) among the first-row 3d-transition metals would effectively decrease the elastic energy of Sr dopant in (La,Sr)BO_3 perovskites.[97] However, doping of the suggested transition metals at the B site also facilitates the formation of oxygen vacancies at the surface, which can cause the electrostatic attraction of Sr atoms toward the surface. This indicates that elastic and electrostatic interactions can often have opposite effects on Sr segregation for partial or total replacement of B-site cations.[34,108] On the other hand, B-site doping may in some cases play a role in reducing both elastic and electrostatic forces. As mentioned above, Koo et al. and Tsvetkov et al. demonstrated that Hf or Zr doping at the B site reduces the extent of Sr enrichment at the surface.[37,106] Although these papers mainly focused on only one aspect of the driving forces of Sr segregation, Hf or Zr doping might affect both elastic and electrostatic interactions in their respective experimental results. Moreover, although above we only discussed the effect of oxygen vacancy on the electrostatic interaction, the formation of oxygen vacancy can also contribute to the elastic interaction via chemical expansion or contraction.[35] Upon oxygen vacancy formation in oxide materials, the superposition of lattice contraction around an oxygen vacancy and lattice expansion caused by ionic radius change can lead to chemical expansion or contraction, generating mechanical stresses.[109,110] Experimental evidence of chemical expansion or of a contraction effect on Sr segregation was observed by changes in the lattice parameter as a function of oxygen pressure. Lee et al. showed that the large lattice expansion under low oxygen pressure decreased the elastic interaction and accordingly reduced the Sr segregation in Sr-doped $LaMnO_3$. This result implies that the change in oxygen vacancy concentration can control the elastic interaction as well as the electrostatic interaction.[35] Lastly, in addition to the effect of A-site defects on the elastic interaction, they can also play a crucial role in decreasing the surface charges because the AO surfaces of (La,Sr)BO_3-type perovskites are positively charged as mentioned above. Thus, A-site defects can also change the electrostatic interaction to suppress the Sr segregation.[102]

To sum up, from a microscopic standpoint, elastic and electrostatic interactions are the major driving forces of Sr segregation (Figure 5D). Previous papers have demonstrated that each effect can be tuned by doping or lattice strain. However, to effectively inhibit Sr segregation it is necessary to find ways to simultaneously control or

optimize both the elastic and electrostatic interactions, because the two effects are difficult to completely decouple from each other. Apart from this, the atomic arrangements at the surface can be influenced by various factors such as atmosphere, temperature, polarization, lattice structure, composition, defects, and so on. In any case, they may partly contribute to the driving forces that rearrange the surface or bulk atoms for cation segregation. As reviewed so far, many theories have been proposed or developed to understand segregation phenomena. Although multiple studies have suggested certain descriptors to predict the cation segregation under certain limited conditions, no universal driving force that can be generally applied to all perovskite-based materials has yet been identified due to the complexity of segregation phenomena. Therefore, more fundamental studies of the origin of cation segregation and the effect of external environment on the segregation are required. It should be noted that A-site segregation phenomena have also been observed for double perovskite ($GdBaCo_2O_{5+\delta}$), RP ($La_2NiO_{4+\delta}$), and Aurivillius (Bi_2MoO_6, Bi_2O_2 [$A_{n-1}B_nO_{3n+1}$]).[30,48,49] These phases of oxides related to the perovskites would also experience the electrostatic interaction due to the surface charges as well as the elastic interaction caused by the size mismatch between the host and dopant cations. We therefore believe that the two interactions constitute the key contributions to the cation segregation for the related oxides, and a similar argument with regard to the perovskites can be made. However, because there may be other specific contributions to the cation segregation for these types of materials, more systematic and detailed studies are necessary in the future.

Other Contributions to Sr Segregation

So far, we have discussed two key factors that segregate dopant or constituent Sr atoms to the surface. Advances in computational material science have made it possible to incorporate classic theories (i.e., Langmuir-McLean isotherm) into the interpretation of phenomena related to perovskite oxides, which are a complicated multicomponent system of ionic bonds.[98] The discussion above is, however, limited to the driving forces that cause the atomic rearrangement at the outermost surface based on energetics at finite temperatures. On the other hand, Sr segregation, which is mainly observed in SOC electrodes, involves the separation of the composition on a macroscopic scale (i.e., at distances greater than 10 nm), not only on the Sr coverage change of the outermost surface.[11–26] Therefore, it is obvious that a description from a macroscopic standpoint is also needed to elucidate the Sr segregation, especially at high temperatures. Here, we discuss two other factors that have been reported in the literature as governing the surface Sr excess. The first is kinetic demixing caused by the thermodynamic potential gradient; the second is the formation of Sr vacancies according to temperature and oxygen partial pressure, which would act as a source of Sr.

In oxides containing multiple cations, differences in the transport rates of charged ions can allow more of one ion to build up at the sink (or source) than another, thus leading to compositional separation during ambipolar diffusion. Kinetic demixing is defined as the compositional separation of an initially homogeneous material due to differential atomic transport rates under a common driving force.[112] This driving force may be a gradient in oxygen potential, electrical potential, stress, temperature, or other factors. Indeed, the kinetic demixing of perovskite oxides under an oxygen potential gradient has been observed by many researchers.[21,113–119] When the material is exposed to an oxygen potential gradient, the chemical affinity for oxygen causes the cations to migrate toward the higher pO_2 side, and the faster cations are enriched on the high-oxygen surfaces. For example, Lein et al. observed rapid compositional changes and decomposition on the surface of

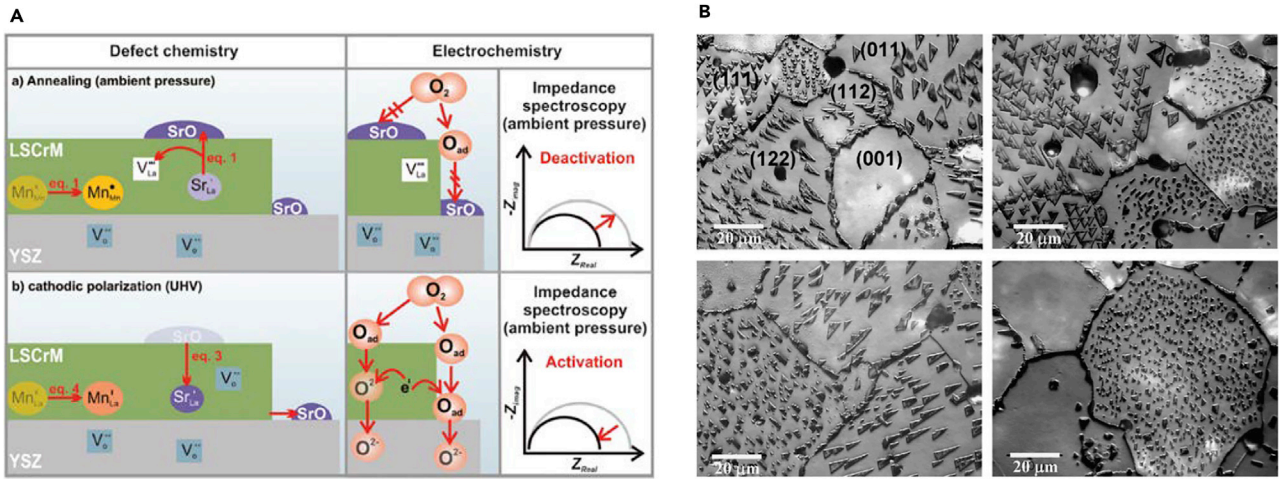

Figure 6. Other Factors Controlling Sr Segregation

(A) The effect of polarization on defect chemistry and surface activity of $La_{0.75}Sr_{0.25}Cr_{0.5}Mn_{0.5}O_{3\pm\delta}$ (LSCrM)/Y_2O_3-stabilized ZrO_2 (YSZ) electrode. In the case of cathodic polarization, the segregated surface Sr is dissolved in the parent perovskite matrix and the passivating SrO secondary phases are removed. Reprinted from Huber et al.,[124] with permission. Copyright 2012, Royal Society of Chemistry.

(B) Optical micrograph images of the reoxidized surface of polycrystalline $SrTi_{0.95}Nb_{0.05}O_3$ at 1,200°C for 30 hr in air. Depending on the orientation of the grains, islands of different shapes, sizes, area, density, and lateral direction are formed. Reprinted from Rahmati et al.,[45] with permission. Copyright 2005, Elsevier.

a $La_{0.5}Sr_{0.5}Co_{0.5}Fe_{0.5}O_{3-\delta}$ membrane when it was used for a long time for oxygen permeation. The difference in cation mobility was demonstrated by the accumulation of Sr/La- or Co/Fe-rich phase on the surface of $La_{0.5}Sr_{0.5}Co_{0.5}Fe_{0.5}O_{3-\delta}$ exposed to various oxygen partial pressures.[113] Similarly, Oh et al. reported that many particles containing Sr and Co were formed by compositional changes when the surface of $La_{0.6}Sr_{0.4}Co_{0.2}Fe_{0.8}O_{3-\delta}$ was exposed to high oxygen partial pressure.[114] It has also been suggested that other thermodynamic driving forces, besides the oxygen potential gradient, may lead to compositional separation near the surface of Sr-containing perovskite oxides. Huber et al. used XPS measurement to investigate the effects of electrochemical activation on the surface composition of $La_{0.75}Sr_{0.25}Cr_{0.5}Mn_{0.5}O_{3\pm\delta}$ at 600°C. Anodic polarization at +2.0 V led to a further acceleration of the Sr excess on the surfaces, whereas it was suppressed after cathodic polarization treatment (Figure 6A).[124] Kinetic demixing has also been suggested by reports that excess Sr on the perovskite-based O_2 electrode surface increases with the cell current density.[120,121] On the other hand, Wang et al. have shown that the density of dislocations is unusually high near the surface of cut and unannealed $SrTiO_3$ single crystals. They suggested that these extended defects not only serve as fast diffusion paths for cations, predominantly Sr, within the near-surface region, but also they are accompanied by a strained region.[122] This may be sufficient for the local mechanical stress gradients to drive the segregation of cations. Using AFM and energy-dispersive X-ray spectroscopy measurements, Szot et al. reported evidence for this on mechanically deformed single-crystal $SrTiO_3$ surfaces at elevated temperatures. They concluded that mechanical stress caused massive segregation of Sr and subsequent recrystallization at the surface.[70,71]

These observations suggest that the surface of the perovskite SOC O_2 electrode becomes enriched in Sr during the process of kinetic demixing. It is noteworthy, however, that only very few studies have reported on kinetic demixing in SOC electrodes. For example, the complexity of the structure and operating conditions of SOC electrodes make it difficult to determine what kind of driving force exists

around the electrodes and how large they are. Certainly, there is a large electrochemical overpotential near the surface of SOC electrodes in operation. In addition, due to the difference in thermal and chemical expansion between the electrode and the electrolyte (or the current collector), a large stress may be applied to the electrode. However, the detailed profile of the electric potential or stress around an actual working electrode is not well known. Moreover, information on the transport characteristics of the cations constituting perovskite oxides is very limited, and the cation diffusion mechanism in a given structure and composition still remains an open question, especially for relatively low temperatures below 1,000°C and for defective paths, such as those at GBs. Therefore, it is necessary to confirm the thermodynamic potential distribution according to the operating conditions and the electrode structure, or to analyze the compositional profile near the surface under a precisely controlled potential gradient. Studies to identify the cation diffusion mechanism through the grain boundary and observe the nucleation and growth dynamics of the Sr-rich phase on the surface are also required to understand the impact of demixing on surface Sr segregation.

Next, from the point of view of defect chemistry, Sr enrichment and the resulting formation of SrO at perovskite oxide surfaces can be understood as the result of a partial Schottky defect formation reaction. To form SrO on the surface, Sr and O atoms in the oxide lattice must be pulled out one by one to the surface, as expressed in the following equation:

$$Sr_{Sr}^{\times} + O_{O}^{\times} \rightleftharpoons V_{Sr}'' + V_{O}^{\bullet\bullet} + SrO_{surf}.$$

In this case, the higher the temperature and hence the more mobile the Sr vacancies, the more active the partial Schottky reaction. Thus, the formation of Sr vacancies and the consequent supply of Sr to the surface can also facilitate the Sr segregation. Rahmati et al. observed Sr-rich islands on the surface of initially reduced Nb-doped $SrTiO_3$ (5 at%) after high-temperature oxidation (1,200°C for 30 hr). They argued that the islands are formed due to a compensation mechanism in donor-doped $SrTiO_3$ from electrons to Sr vacancies by oxidizing annealing, as shown in Figure 6B.[45] Likewise, Balachandran and Eror reported the formation of RP phase on the surface of 0.1–0.2 at% La-doped $SrTiO_3$ at a high-oxygen partial pressure. They suggested that extra Sr due to Sr vacancies, compensated for by the additional charge of the La, may combine with oxygen to form SrO layers under high-oxygen partial pressure conditions.[46] It is noteworthy that equilibrium constants for various defect reactions in perovskite oxides have rarely been reported, but these constants are unlikely to produce sufficient bulk Sr vacancies to cover the surface with Sr at the relatively low temperatures of SOC operation (<800°C). However, the partial Schottky reaction can be more active at the surface or interface of an electrode, which is a relatively defective region, and this type of factor cannot be ignored.

Lastly, although not considered thus far, it is important to note that the sintering process, a key step during the fabrication of SOC electrodes, can have a significant impact on the Sr segregation phenomenon, as it occurs at a much higher temperature (>1,000°C) than the temperature at which the SOCs operate (<750°C). The sintering process determines the densification and grain growth of the electrode material. It is generally known that the higher the sintering temperature, the higher the conductivity and mechanical strength of the electrode and the stronger the adhesion between the electrode and the electrolyte. On the other hand, a high sintering temperature reduces the porosity and thus the density of triple-phase boundaries, which may have deleterious effects on the electrode performance. This is also the most common cause of mechanical failures during the cell and stack fabrication process.

Therefore, there is always a tradeoff between the materials and the manufacturing process when determining the sintering temperature, and many studies have reported change of the electrode or cell performance outcomes according to the sintering temperature.[125,126] Surprisingly, however, none of these prior studies discussed how the sintering temperature affects the degree of Sr segregation and, thus, deterioration of electrode performance. Sintering takes place only for a short time within a few hours at higher temperatures while the operating temperature of the cell is relatively low but lasts for a very long time, possibly under a strong thermodynamic potential gradient. Therefore, it is not easy to separate the contributions of surface excess Sr from either the sintering process or the operating process, and related systematic studies are necessary in the future.

Concluding Remarks

For the rational design of highly efficient and durable perovskite-based SOC O_2-electrode materials, a comprehensive understanding of each factor affecting surface Sr enrichment is required over a wide range of operational environments. We summarize seven key design strategies for long-term stability of Sr-based perovskite materials by suppressing the Sr segregation.

(1) Applying external strain can be an effective way to control Sr segregation (Figure 7A). However, depending on the composition of the material, the influence of the applied strain on the segregation will vary greatly. We believe that the perovskite composition determines whether the lattice should be stretched or compressed to suppress Sr segregation. Therefore, further investigation is required to search for the optimal degree and direction of the applied strain, which would induce different responses for each material. Note that it is virtually impossible to apply direct pressure (or strain) to the electrode in operation, which only helps to clarify the cause of Sr segregation at the atomistic level, allowing us to prepare the strategy (2) below.

(2) The substitution of isovalent A- or B-site cations with different ionic radii could be a practical way to apply effective strain for the reduction of the stress near Sr. This substitution stabilizes elemental Sr within the perovskite lattice and suppresses its segregation (Figure 7B). In this case, as in (1), the appropriate ionic radius of the dopant for suppressing Sr segregation will vary depending on the composition of the perovskite. Moreover, the addition of a dopant may change the bulk characteristics of the material itself, and thus further investigation is required to comprehensively observe the transport, catalytic, and defect properties, along with the surface composition.

(3) The modification of surfaces with more and less-reducible cations than those of the host can reduce Sr segregation by changing the electrostatic interaction between surface oxygen vacancies and cations (Figure 7C). To achieve high surface kinetics, as well as stability, it is therefore essential to find the optimal surface reducibility. It is also necessary to investigate the proper choice of cation and coating method for the surface modification.

(4) Using the nonstoichiometric perovskite with $A/B < 1$ is also a possible way to alleviate Sr segregation (Figure 7D). A-site defects can effectively reduce both elastic and electrostatic interactions that cause the segregation. Although a small amount of A-site defects could increase the valence states of B-site cations, thereby enhancing the stability of BO_6 octahedral, the excess of A-site defects may significantly decrease the phase stability of perovskite. It is therefore important to optimize the amount of A-site defects to suppress Sr segregation while maintaining the structural stability.

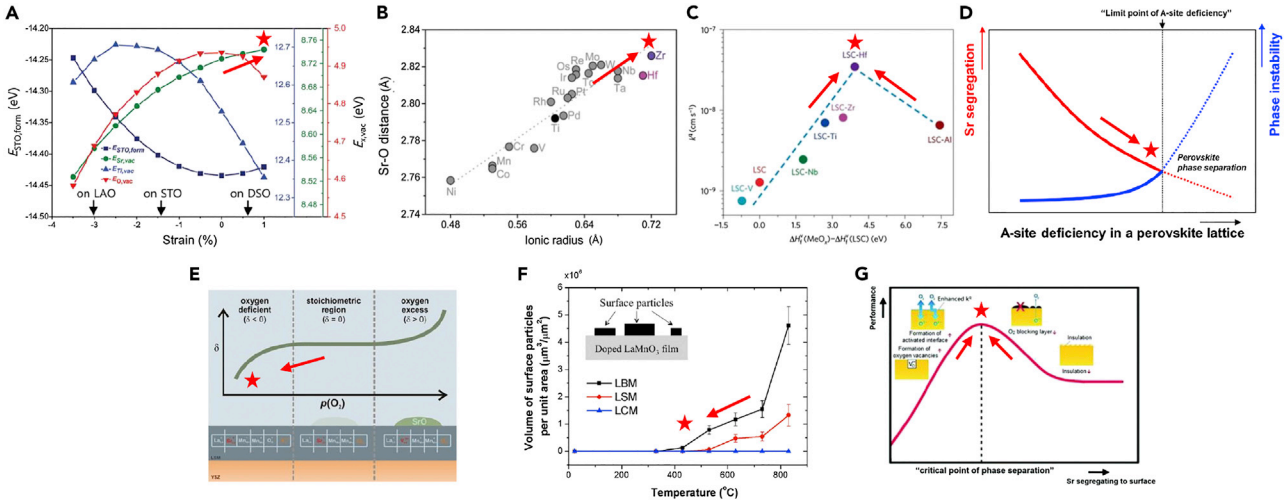

Figure 7. Optimal Conditions to Suppress Sr Segregation

(A) Strain-dependent energetics of each element in $SrTiO_3$ (STO). $E_{STO,\,form}$ and $E_{X,vac}$ (X = Ti, O, and Sr) are the formation energy of STO and the vacancy formation energy of each element in bulk STO, respectively. Reprinted from Koo et al.,[37] with permission. Copyright 2018, Royal Society of Chemistry.

(B) The linear relationship between the ionic radius of transition metal dopant and the DFT-optimized bond length of Sr-O in $SrTi_{0.25}TM_{0.25}Fe_{0.50}O_3$. Reprinted from Koo et al.,[37] with permission. Copyright 2018, Royal Society of Chemistry.

(C) Volcano-like plot between the enthalpy of oxygen vacancy formation (ΔH^{v}_{f}) in the binary oxides (MeO_x) and the oxygen surface exchange kinetics of $La_{0.8}Sr_{0.2}CoO_{3-\delta}$ (LSC)-Me. Reprinted from Tsvetkov et al.,[106] with permission. Copyright 2016, Springer Nature.

(D) Schematic of the correlation between Sr segregation and phase stability of A-site depleted perovskite oxide.

(E) Schematic of the oxygen stoichiometry of $(La_{0.8}Sr_{0.2})_{0.92}MnO_{3-\delta}$ phase and SrO formation as a function of oxygen partial pressure. Reprinted from Huber et al.,[16] with permission. Copyright 2012, Elsevier.

(F) Volume per unit area of the segregated cation particles as a function of annealing temperature for Ca-, Sr-, and Ba-doped $LaMnO_3$. Reprinted from Lee et al.,[35] with permission. Copyright 2013, American Chemical Society.

(G) Schematic of "critical point of phase separation" hypothesis for the correlation between Sr segregation and electrode performance in Sr-doped $LaCoO_3$. Reprinted from Li et al.,[41] with permission. Copyright 2017, Royal Society of Chemistry.

The arrow and star indicate ideal direction and point to suppress Sr segregation in each condition.

(5) The Sr segregation at the perovskite-based electrode surface can be controlled to some extent by changing the oxygen partial pressure and the applied voltage. Applying a cathodic and anodic bias to the electrode at high temperatures had an effect similar to increasing or decreasing the oxygen partial pressure, respectively, in terms of the effective oxygen vacancy concentration. In fact, applying cathodic bias (or lowering pO_2) appears to help suppress Sr segregation either by releasing the stresses around Sr or by inhibiting selective demixing of Sr toward the perovskite surface (Figure 7E). In this regard, the cathodic bias may be applied intermittently to reverse the Sr segregation to the extent that it is reversible. Studies to develop a new operating logic to mitigate the Sr segregation under dynamic electrical loads are necessary.

(6) An increase in temperature typically activates Sr segregation thermodynamically and kinetically. Therefore, lowering the operating temperature of SOCs will be an effective way to suppress the segregation (Figure 7F). In fact, the development of lower-temperature operation SOCs is also a current trend in related fields to reduce cost associated with cell fabrication and operation. Lowering the sintering temperature is also worth considering in this regard if the mechanical integrity and adhesion of the electrode can be maintained.

(7) The formation of a new composition in the near-surface region upon Sr segregation may play an important role in the electrode performance. However, it is still unclear which phases or hetero-interfaces are formed on the surface at

the critical point of Sr segregation, and what their role is on the electrode surfaces (Figure 7G). Therefore, the application of surface analytic techniques with high chemical and spatial resolution will be required.

We believe that these strategies for electrode design will also be applicable to the suppression of other kinds of cation segregation, such as that of Pb in $La_{0.65}Pb_{0.35}MnO_{3-\delta}$ and Ba in $Ba_{0.5}Sr_{0.5}Co_{0.8}Fe_{0.2}O_{3-\delta}$.[31,32] In addition to the factors that influence the Sr segregation mentioned thus far there are many other factors to be investigated, such as nucleation/growth kinetics of secondary phases, interfacial reaction with electrolytes or interconnects, surface impurity contamination, and so on.[77,123] More research is therefore necessary to optimize overall cell efficiency and stability. Fortunately, with the help of recent advanced experimental and theoretical approaches, it is possible to analyze the origin of cation segregation and its effects on SOC performance with greater sophistication. For example, it is now possible to trace the surface reaction or ionic movement in real time via *in situ* experiments and look into the phenomena in detail at the atomic scale via advanced theoretical modeling and simulation techniques. In the near future, based on the insights provided by this review, these state-of-the-art experiments and/or theoretical analyses will allow us to design further enhanced electrode materials for SOCs.

ACKNOWLEDGMENTS

This study was supported by the Samsung Research Funding Center for Future Technology (SRFC-MA1502-13).

REFERENCES

1. Peña, M.A., and Fierro, J.L.G. (2001). Chemical structures and performance of perovskite oxides. Chem. Rev. *101*, 1981–2017.

2. Cao, R., Lee, J.-S., Liu, M., and Cho, J. (2012). Recent progress in non-precious catalysts for metal-air batteries. Adv. Energy Mater. *2*, 816–829.

3. Bousquet, E., Dawber, M., Stucki, N., Lichtensteiger, C., Hermet, P., Gariglio, S., Triscone, J.-M., and Ghosez, P. (2008). Improper ferroelectricity in perovskite oxide artificial superlattices. Nature *452*, 732–736.

4. Homes, C.C., Vogt, T., Shapiro, S.M., Wakimoto, S., and Ramirez, A.P. (2001). Optical response of high-dielectric-constant perovskite-related oxide. Science *293*, 673–676.

5. Shao, Z., and Haile, S.M. (2004). A high-performance cathode for the next generation of solid-oxide fuel cells. Nature *431*, 170–173.

6. McDaniel, A.H., Miller, E.C., Arifin, D., Ambrosini, A., Coker, E.N., O'Hayre, R., Chueh, W.C., and Tong, J. (2013). Sr- and Mn-doped $LaAlO_{3-\delta}$ for solar thermochemical H_2 and CO production. Energy Environ. Sci. *6*, 2424–2428.

7. Grinberg, I., West, D.V., Torres, M., Gou, G., Stein, D.M., Wu, L., Chen, G., Gallo, E.M., Akbashev, A.R., Davies, P.K., et al. (2013). Perovskite oxides for visible-light-absorbing ferroelectric and photovoltaic materials. Nature *503*, 509–512.

8. Maeno, Y., Hashimoto, H., Yoshida, K., Nishizaki, S., Fujita, T., Bednorz, J.G., and Lichtenberg, F. (1994). Superconductivity in a layered perovskite without copper. Nature *372*, 532–534.

9. Nishihata, Y., Mizuki, J., Akao, T., Tanaka, H., Uenishi, M., Kimura, M., Okamoto, T., and Hamada, N. (2002). Self-regeneration of a Pd-perovskite catalyst for automotive emissions control. Nature *418*, 164–167.

10. Grabowska, E. (2016). Selected perovskite oxides: characterization, preparation and photocatalytic properties-a review. Appl. Catal. B *186*, 97–126.

11. Cai, Z., Kubicek, M., Fleig, J., and Yildiz, B. (2012). Chemical heterogeneities on $La_{0.6}Sr_{0.4}CoO_{3-\delta}$ thin films-correlations to cathode surface activity and stability. Chem. Mater. *24*, 1116–1127.

12. Kubicek, M., Limbeck, A., Frömling, T., Hutter, H., and Fleig, J. (2011). Relationship between cation segregation and the electrochemical oxygen reduction kinetics of $La_{0.6}Sr_{0.4}CoO_{3-\delta}$ thin film electrodes. J. Electrochem. Soc. *158*, B727–B734.

13. Jiang, S.P., and Love, J.G. (2001). Origin of the initial polarization behavior of Sr-doped $LaMnO_3$ for O_2 reduction in solid oxide fuel cells. Solid State Ion. *138*, 183–190.

14. Choi, S., Yoo, S., Kim, J., Park, S., Jun, A., Sengodan, S., Kim, J., Shin, J., Jeong, H.Y., Choi, Y., et al. (2013). Highly efficient and robust cathode materials for low-temperature solid oxide fuel cells: $PrBa_{0.5}Sr_{0.5}Co_{2-x}Fe_xO_{5+\delta}$. Sci. Rep. *3*, 2426.

15. Pan, Z., Liu, Q., Zhang, L., Zhang, X., and Chan, S.H. (2015). Effect of Sr surface segregation of $La_{0.6}Sr_{0.4}Co_{0.2}Fe_{0.8}O_{3-\delta}$ electrode on its electrochemical performance in SOC. J. Electrochem. Soc. *162*, F1316–F1323.

16. Huber, A.-K., Falk, M., Rohnke, M., Juerssen, B., Amati, M., Gregoratti, L., Hesse, D., and Janek, J. (2012). In situ study of activation and de-activation of LSM fuel cell cathodes—electrochemistry and surface analysis of thin-film electrodes. J. Catal. *294*, 79–88.

17. Chen, Y., Jung, W., Cai, Z., Kim, J.J., Tuller, H.L., and Yildiz, B. (2012). Impact of Sr segregation on the electronic structure and oxygen reduction activity of $SrTi_{1-x}Fe_xO_3$ surfaces. Energy Environ. Sci. *5*, 7979–7988.

18. Rupp, G.M., Opitz, A.K., Nenning, A., Limbeck, A., and Fleig, J. (2017). Real-time impedance monitoring of oxygen reduction during surface modification of thin film cathodes. Nat. Mater. *16*, 640–646.

19. Nenning, A., Opitz, A.K., Rameshan, C., Rameshan, R., Blume, R., Hävecker, M., Knop-Gericke, A., Rupprechter, G., Klötzer, B., and Fleig, J. (2016). Ambient pressure XPS study of mixed conducting perovskite-type SOFC cathode and anode materials under well-defined electrochemical polarization. J. Phys. Chem. C *120*, 1461–1471.

20. Rupp, G.M., Téllez, H., Druce, J., Limbeck, A., Ishihara, T., Kilner, J., and Fleig, J. (2015).

Surface chemistry of $La_{0.6}Sr_{0.4}CoO_{3-\delta}$ thin films and its impact on the oxygen surface exchange resistance. J. Mater. Chem. A *3*, 22759–22769.

21. Jung, W., and Tuller, H.L. (2012). Investigation of surface Sr segregation in model thin film solid oxide fuel cell perovskite electrodes. Energy Environ. Sci. *5*, 5370–5378.

22. Crumlin, E.J., Mutoro, E., Liu, Z., Grass, M.E., Biegalski, M.D., Lee, Y.-L., Morgan, D., Christen, H.M., Bluhm, H., and Shao-Horn, Y. (2012). Surface strontium enrichment on highly active perovskites for oxygen electrocatalysis in solid oxide fuel cells. Energy Environ. Sci. *5*, 6081–6088.

23. Mutoro, E., Crumlin, E.J., Biegalski, M.D., Christen, H.M., and Shao-Horn, Y. (2011). Enhanced oxygen reduction activity on surface-decorated perovskite thin films for solid oxide fuel cells. Energy Environ. Sci. *4*, 3689–3696.

24. Chen, Y., Téllez, H., Burriel, M., Yang, F., Tsvetkov, N., Cai, Z., McComb, D.W., Kilner, J.A., and Yildiz, B. (2015). Segregated chemistry and structure on (001) and (100) surfaces of $(La_{1-x}Sr_x)_2CoO_4$ override the crystal anisotropy in oxygen exchange kinetics. Chem. Mater. *27*, 5436–5450.

25. Crumlin, E.J., Mutoro, E., Hong, W.T., Biegalski, M.D., Christen, H.M., Liu, Z., Bluhm, H., and Shao-Horn, Y. (2013). In situ ambient pressure X-ray photoelectron spectroscopy of cobalt perovskite surfaces under cathodic polarization at high temperatures. J. Phys. Chem. C *117*, 16087–16094.

26. Lee, W., and Yildiz, B. (2013). Factors that influence cation segregation at the surfaces of perovskite oxides. ECS Trans. *57*, 2115–2123.

27. Kwon, O., Sengodan, S., Kim, K., Kim, G., Jeong, H.Y., Shin, J., Ju, Y.-W., Han, J.W., and Kim, G. (2017). Exsolution trends and co-segregation aspects of self-grown catalyst nanoparticles in perovskites. Nat. Commun. *8*, 15967.

28. Neagu, D., Tsekouras, G., Miller, D.N., Ménard, H., and Irvine, J.T.S. (2013). In situ growth of nanoparticles through control of non-stoichiometry. Nat. Chem. *5*, 916–923.

29. Myung, J.-H., Neagu, D., Miller, D.N., and Irvine, J.T.S. (2016). Switching on electrocatalytic activity in solid oxide cells. Nature *537*, 528–531.

30. Druce, J., Téllez, H., Burriel, M., Sharp, M.D., Fawcett, L.J., Cook, S.N., Mcphail, D.S., Ishihara, T., Brongersma, H.H., and Kilner, J.A. (2014). Surface termination and subsurface restructuring of perovskite-based solid oxide electrode materials. Energy Environ. Sci. *7*, 3593–3599.

31. Borca, C.N., Xu, B., Komesu, T., Jeong, H.-K., Liu, M.T., Liou, S.H., and Dowben, P.A. (2002). The surface phases of the $La_{0.65}Pb_{0.35}MnO_3$ manganese perovskite surface. Surf. Sci. *512*, L346–L352.

32. van Veen, A.C., Rebeilleau, M., Farrusseng, D., and Mirodatos, C. (2003). Studies on the performance stability of mixed conducting BSCFO membranes in medium temperature oxygen permeation. Chem. Commun. (Camb.) *33*, 32–33.

33. Cai, Z., Kuru, Y., Han, J.W., Chen, Y., and Yildiz, B. (2011). Surface electronic structure transitions at high temperature on perovskite oxides: the case of strained $La_{0.8}Sr_{0.2}CoO_3$ thin films. J. Am. Chem. Soc. *133*, 17696–17704.

34. Jalili, H., Han, J.W., Kuru, Y., Cai, Z., and Yildiz, B. (2011). New insights into the strain coupling to surface chemistry, electronic structure, and reactivity of $La_{0.7}Sr_{0.3}MnO_3$. J. Phys. Chem. Lett. *3*, 801–807.

35. Lee, W., Han, J.W., Chen, Y., Cai, Z., and Yildiz, B. (2013). Cation size mismatch and charge interactions drive dopant segregation at the surfaces of manganite perovskite. J. Am. Chem. Soc. *135*, 7909–7925.

36. Yu, Y., Ludwig, K.F., Woicik, J.C., Gopalan, S., Pal, U.B., Kaspar, T.C., and Basu, S.N. (2016). Effect of Sr content and strain on Sr surface segregation of $La_{1-x}Sr_xCo_{0.2}Fe_{0.8}O_{3-\delta}$ as cathode material for solid oxide fuel cells. ACS Appl. Mater. Interfaces *8*, 26704–26711.

37. Koo, B., Kwon, H., Kim, Y., Seo, H.G., Han, J.W., and Jung, W. (2018). Enhanced oxygen exchange of perovskite oxide surfaces through strain-driven chemical stabilization. Energy Environ. Sci. *11*, 71–77.

38. Koo, J.Y., Kwon, H., Ahn, M., Choi, M., Son, J.-W., Han, J.W., and Lee, W. (2018). Suppression of cation segregation in (La,Sr)$CoO_{3-\delta}$ by elastic energy minimization. ACS Appl. Mater. Interfaces *10*, 8057–8065.

39. Chen, Y., Zhou, W., Ding, D., Liu, M., Ciucci, F., Tade, M., and Shao, Z. (2015). Advances in cathode materials for solid oxide fuel cells: complex oxides without alkaline earth metal elements. Adv. Energy Mater. *5*, 1–34.

40. Irvine, J.T.S., Neagu, D., Verbraeken, M.C., Chatzichristodoulou, C., Graves, C., and Mogensen, M.B. (2016). Evolution of the electrochemical interface in high-temperature fuel cells and electrolysers. Nat. Energy *1*, 1–13.

41. Li, Y., Zhang, W., Zheng, Y., Chen, J., Yu, B., Chen, Y., and Liu, M. (2017). Controlling cation segregation in perovskite-based electrodes for high electro-catalytic activity and durability. Chem. Soc. Rev. *46*, 6345–6378.

42. Bachelet, R., Sanchez, F., Palomares, F.J., Ocal, C., and Fontcuberta, J. (2009). Atomically flat SrO-terminated $SrTiO_3$(001) substrate. Appl. Phys. Lett. *95*, 141915.

43. Szot, K., Speier, W., Breuer, U., Meyer, R., Szade, J., and Waser, R. (2000). Formation of micro-crystals on the (100) surface of $SrTiO_3$ at elevated temperatures. Surf. Sci. *460*, 112–128.

44. Niania, M.A., Podor, R., Skinner, S.J., and Kilner, J.A. (2015). In-situ surface analysis of SOFC cathode degradation using high temperature environmental scanning electron microscopy. ECS Trans. *68*, 665–670.

45. Rahmati, B., Fleig, J., Sigle, W., Bischoff, E., Maier, J., and Rühle, M. (2005). Oxidation of reduced polycrystalline Nb-doped $SrTiO_3$: characterization of surface islands. Surf. Sci. *595*, 115–126.

46. Balachandran, U., and Eror, N.G. (1982). Electrical conductivity in lanthanum-doped strontium titanate. J. Electrochem. Soc. *129*, 1021–1026.

47. Szot, K., Freiburg, C., and Pawelczyk, M. (1991). Layer structures BaO-$BaTiO_3$ in the region of p-type conductivity on the surface of $BaTiO_3$. Appl. Phys. A *53*, 563–567.

48. Kendall, K.R., Navas, C., Thomas, J.K., and Zur Loye, H.-C. (1996). Synthesis and ionic conductivity of a new series of modified Aurivillius phases. Chem. Mater. *8*, 642–649.

49. Watanabe, K., Hartmann, A.J., Lamb, R.N., Craig, R.P., Thurgate, S.M., and Scott, J.F. (2000). Valence band and bandgap states of ferroelectric $SrBi_2Ta_2O_9$ thin films. Jpn. J. Appl. Phys. *39*, 309–311.

50. Schmalzried, H. (1983). Internal and external oxidation of nonmetallic compounds and solid solution (I). Ber. Bunsenges. Phys. Chem. *87*, 551–558.

51. Gorte, R.J., and Vohs, J.M. (2011). Catalysis in solid oxide fuel cells. Annu. Rev. Chem. Biomol. Eng. *2*, 9–30.

52. Graves, C., Ebbesen, S.D., Jensen, S.H., Simonsen, S.B., and Mogensen, M.B. (2015). Eliminating degradation in solid oxide electrochemical cells by reversible operation. Nat. Mater. *14*, 239–244.

53. Mahato, N., Banerjee, A., Gupta, A., Omar, S., and Balani, K. (2015). Progress in material selection for solid oxide fuel cell technology: a review. Prog. Mater. Sci. *72*, 141–337.

54. Ni, M., Leung, M.K.H., and Leung, D.Y.C. (2008). Technological development of hydrogen production by solid oxide electrolyzer cell (SOEC). Int. J. Hydrogen Energy *33*, 2337–2354.

55. Wachsman, E.D., and Lee, K.T. (2011). Lowering the temperature of solid oxide fuel cells. Science *334*, 935–939.

56. Shearing, P.R., Brett, D.J.L., and Brandon, N.P. (2010). Towards intelligent engineering of SOFC electrodes: a review of advanced microstructural characterisation techniques. Int. Mater. Rev. *55*, 347–363.

57. Sun, C., Hui, R., and Roller, J. (2010). Cathode materials for solid oxide fuel cells: a review. J. Solid State Electrochem. *14*, 1125–1144.

58. Jacobson, A.J. (2010). Materials for solid oxide fuel cells. Chem. Mater. *22*, 660–674.

59. Adler, S.B. (2004). Factors governing oxygen reduction in solid oxide fuel cell cathodes. Chem. Rev. *104*, 4791–4843.

60. Petrov, A.N., Kononchuk, O.F., Andreev, A.V., Cherepanov, V.A., and Kofstad, P. (1995). Crystal structure, electrical and magnetic properties of $La_{1-x}Sr_xCoO_{3-y}$. Solid State Ion. *80*, 189–199.

61. Bongio, E.V., Black, H., Raszewski, F.C., Edwards, D., McConville, C.J., and Amarakoon, V.R.W. (2005). Microstructural and high-temperature electrical characterization of $La_{1-x}Sr_xFeO_{3-\delta}$. Fuel Cells *14*, 193–198.

62. Mizusaki, J. (1992). Nonstoichiometry, diffusion, and electrical properties of perovskite-type oxide electrode materials. Solid State Ion. *52*, 79–91.

63. Digiuseppe, G., and Sun, L. (2011). Electrochemical performance of a solid oxide fuel cell with an LSCF cathode under different oxygen concentrations. Int. J. Hydrogen Energy *36*, 5076–5087.

64. Tietz, F., Arul Raj, I., Zahid, M., and Stöver, D. (2006). Electrical conductivity and thermal expansion of $La_{0.8}Sr_{0.2}(Mn,Fe,Co)O_{3-\delta}$ perovskites. Solid State Ion. *177*, 1753–1756.

65. Caillol, N., Pijolat, M., and Siebert, E. (2007). Investigation of chemisorbed oxygen, surface segregation and effect of post-treatments on $La_{0.8}Sr_{0.2}MnO_3$ powder and screen-printed layers for solid oxide fuel cell cathodes. Appl. Surf. Sci. *253*, 4641–4648.

66. Mikkelsen, L., Andersen, I.G.K., and Skou, E.M. (2002). Oxygen transport in $La_{1-x}Sr_xFe_{1-y}Mn_yO_{3-\delta}$ perovskites. Solid State Ion. *152-153*, 703–707.

67. Yang, G., Zhou, W., Liu, M., and Shao, Z. (2016). Enhancing electrode performance by exsolved nanoparticles: a superior cobalt-free perovskite electrocatalyst for solid oxide fuel cells. ACS Appl. Mater. Interfaces *8*, 35308–35314.

68. Suntivich, J., Gasteiger, H.A., Yabuuchi, N., Nakanishi, H., Goodenough, J.B., and Shao-Horn, Y. (2011). Design principles for oxygen-reduction activity on perovskite oxide catalysts for fuel cells and metal-air batteries. Nat. Chem. *3*, 546–550.

69. McLean, D. (1957). Grain Boundaries in Metals (Clarendon Press).

70. Szot, K., Speier, W., Herion, J., and Freiburg, C.H. (1997). Restructuring of the surface region in $SrTiO_3$. Appl. Phys. A *64*, 55–59.

71. Szot, K., and Speier, W. (1999). Surfaces of reduced and oxidized $SrTiO_3$ from atomic force microscopy. Phys. Rev. B *60*, 5909–5926.

72. Dulli, H., Dowben, P.A., Liou, S.H., and Plummer, E.W. (2000). Surface segregation and restructuring of colossal-magnetoresistant manganese perovskites $La_{0.65}Sr_{0.35}MnO_3$. Phys. Rev. B *62*, R14629–R14632.

73. Staykov, A., Téllez, H., Akbay, T., Druce, J., Ishihara, T., and Kilner, J. (2015). Oxygen activation and dissociation on transition metal free perovskite surfaces. Chem. Mater. *27*, 8273–8281.

74. Meyer, R., Waser, R., Helmbold, J., and Borchardt, G. (2002). Cationic surface segregation in donor-doped $SrTiO_3$ under oxidizing conditions. J. Electroceram. *9*, 101–110.

75. Wei, H., Beuermann, L., Helmbold, J., Borchardt, G., Kempter, V., Lilienkamp, G., and Maus-Friedrichs, W. (2001). Study of SrO segregation on $SrTiO_3$ (100) surfaces. J. Eur. Ceram. Soc. *21*, 1677–1680.

76. Fullarton, I.C., Jacobs, J.-P., van Benthem, H.E., Kilner, J.A., Brongersma, H.H., Scanlon, P.J., and Steele, B.C.H. (1995). Study of oxygen ion transport in acceptor doped samarium cobalt oxide. Ionics *1*, 51–58.

77. Bucher, E., Sitte, W., Klauser, F., and Bertel, E. (2012). Impact of humid atmospheres on oxygen exchange properties, surface-near elemental composition, and surface morphology of $La_{0.6}Sr_{0.4}CoO_{3-\delta}$. Solid State Ion. *208*, 43–51.

78. Druce, J., Téllez, H., Ishihara, T., and Kilner, J.A. (2015). Oxygen exchange and transport in dual phase ceramic composite electrodes. Faraday Discuss. *182*, 271–288.

79. Feng, Z., Crumlin, E.J., Hong, W.T., Lee, D., Mutoro, E., Biegalski, M.D., Zhou, H., Bluhm, H., Christen, H.M., and Shao-Horn, Y. (2013). In situ studies of the temperature-dependent surface structure and chemistry of single-crystalline (001)-oriented $La_{0.8}Sr_{0.2}CoO_{3-\delta}$ perovskite thin films. J. Phys. Chem. Lett. *4*, 1512–1518.

80. Wu, Q.-H., Liu, M., and Jaegermann, W. (2005). X-ray photoelectron spectroscopy of $La_{0.5}Sr_{0.5}MnO_3$. Mater. Lett. *59*, 1980–1983.

81. Bertacco, R., Contour, J.P., Barthélemy, A., and Olivier, J. (2002). Evidence for strontium segregation in $La_{0.7}Sr_{0.3}MnO_3$ thin films grown by pulsed laser deposition: consequences for tunneling junctions. Surf. Sci. *511*, 366–372.

82. Jiang, S.P. (2015). Thermally and electrochemically induced electrode/electrolyte interfaces in solid oxide fuel cells: an AFM and EIS study. J. Electrochem. Soc. *162*, F1119–F1128.

83. Zhao, L., Drennan, J., Kong, C., Amarasinghe, S., and Jiang, S.P. (2014). Insight into surface segregation and chromium deposition on $La_{0.6}Sr_{0.4}Co_{0.2}Fe_{0.8}O_{3-\delta}$ cathodes of solid oxide fuel cells. J. Mater. Chem. A *2*, 11114–11123.

84. Oh, D., Gostovic, D., and Wachsman, E.D. (2012). Mechanism of $La_{0.6}Sr_{0.4}Co_{0.2}Fe_{0.8}O_3$ cathode degradation. J. Mater. Res. *27*, 1992–1999.

85. Witck, S., and Smyth, D.M. (1984). Variability of the Sr/Ti ratio in $SrTiO_3$. J. Am. Ceram. Soc. *67*, 372–375.

86. Ruddlesden, S.N., and Popper, P. (1958). The compound $Sr_3Ti_2O_7$ and its structure. Acta Cryst. *11*, 54–55.

87. Udayakumar, K.R., and Cormack, A.N. (1989). Non-stoichiometry in alkaline earth excess alkaline earth titanates. J. Phys. Chem. Solids *50*, 55–60.

88. Šturm, S., Rečnik, A., Scheu, C., and Čeh, M. (2000). Formation of Ruddlesden-Popper faults and polytype phases in SrO-doped $SrTiO_3$. J. Mater. Res. *15*, 2131–2139.

89. Friedel, J. (1954). Electronic structure of primary solid solutions in metals. Adv. Phys. *3*, 446–507.

90. Tran, R., Xu, Z., Zhou, N., Radhakrishnan, B., Luo, J., and Ong, S.P. (2016). Computational study of metallic dopant segregation and embrittlement at molybdenum grain boundaries. Acta Mater. *117*, 91–99.

91. Mukherjee, S., and Morán-López, J.L. (1987). Surface segregation in transition-metal alloys and in bimetallic alloy clusters. Surf. Sci. *189–190*, 1135–1142.

92. Wynblatt, P., and Ku, R.C. (1977). Surface energy and solute strain energy effects in surface segregation. Surf. Sci. *65*, 511–531.

93. Desu, S.B., and Payne, D.A. (1990). Interfacial segregation in perovskites: I. Theory. J. Am. Ceram. Soc. *73*, 3398–3406.

94. Williams, F.L., and Boudart, M. (1973). Surface composition of nickel-gold alloys. J. Catal. *30*, 438–443.

95. Løvvik, O.M. (2005). Surface segregation in palladium based alloys from density-functional calculations. Surf. Sci. *583*, 100–106.

96. Han, J.W., Kitchin, J.R., and Sholl, D.S. (2009). Step decoration of chiral metal surfaces. J. Chem. Phys. *130*, 124710.

97. Kwon, H., Lee, W., and Han, J.W. (2016). Suppressing cation segregation on lanthanum-based perovskite oxides to enhance the stability of solid oxide fuel cell cathodes. RSC Adv. *6*, 69782–69789.

98. Piskunov, S., Heifets, E., Jacob, T., Kotomin, E.A., Ellis, D.E., and Spohr, E. (2008). Electronic structure and thermodynamic stability of $LaMnO_3$ and $La_{1-x}Sr_xMnO_3$ (001) surfaces: ab initio calculations. Phys. Rev. B *78*, 1–4.

99. Yoo, S., Jun, A., Ju, Y.-W., Odkhuu, D., Hyodo, J., Jeong, H.Y., Park, N., Shin, J., Ishihara, T., and Kim, G. (2014). Development of double-perovskite compounds as cathode materials for low-temperature solid oxide fuel cells. Angew. Chem. Int. Ed. *53*, 13064–13067.

100. Waller, D., Lane, J.A., Kilner, J.A., and Steele, B.C.H. (1996). The structure of and reaction of A-site deficient $La_{0.6}Sr_{0.4-x}Co_{0.2}Fe_{0.8}O_{3-\delta}$ perovskites. Mater. Lett. *27*, 225–228.

101. Jin, T., and Lu, K. (2011). Surface and interface behaviors of $(La_{0.8}Sr_{0.2})_xMnO_3$ air electrode for solid oxide cells. J. Power Sources *196*, 8331–8339.

102. Ding, H., Virkar, A.V., Liu, M., and Liu, F. (2013). Suppression of Sr surface segregation in $La_{1-x}Sr_xCo_{1-y}Fe_yO_{3-\delta}$: a first principles study. Phys. Chem. Chem. Phys. *15*, 489–496.

103. Guo, X. (1995). Physical origin of the intrinsic grain-boundary resistivity of stabilized-zirconia: role of the space-charge layers. Solid State Ion. *81*, 235–242.

104. Lee, H.B., Prinz, F.B., and Cai, W. (2010). Atomistic simulations of surface segregation of defects in solid oxide electrolytes. Acta Mater. *58*, 2197–2206.

105. Hamada, I., Uozumi, A., Morikawa, Y., Yanase, A., and Katayama-Yoshida, H. (2011). A density functional theory study of self-regenerating catalysts $LaFe_{1-x}M_xO_{3-y}$ (M = Pd, Rh, Pt). J. Am. Chem. Soc. *133*, 18506–18509.

106. Tsvetkov, N., Lu, Q., Sun, L., Crumlin, E.J., and Yildiz, B. (2016). Improved chemical and electrochemical stability of perovskite oxides with less reducible cations at the surface. Nat. Mater. *15*, 1010–1016.

107. Fister, T.T., Fong, D.D., Eastman, J.A., Baldo, P.M., Highland, M.J., Fuoss, P.H., Balasubramaniam, K.R., Meador, J.C., and Salvador, P.A. (2008). In situ characterization

of strontium surface segregation in epitaxial $La_{0.7}Sr_{0.3}MnO_3$ thin films as a function of oxygen partial pressure. Appl. Phys. Lett. *93*, 151904.

108. Lee, Y.L., Kleis, J., Rossmeisl, J., and Morgan, D. (2009). Ab initio energetics of $LaBO_3$ (001) (B=Mn, Fe, Co, and Ni) for solid oxide fuel cell cathodes. Phys. Rev. B *80*, 1–20.

109. Bishop, S.R., Marrocchelli, D., Chatzichristodoulou, C., Perry, N.H., Mogensen, M.B., Tuller, H.L., and Wachsman, E.D. (2014). Chemical expansion: implications for electrochemical energy storage and conversion devices. Annu. Rev. Mater. Res. *44*, 205–239.

110. Marrocchelli, D., Bishop, S.R., and Kilner, J. (2013). Chemical expansion and its dependence on the host cation radius. J. Mater. Chem. A *1*, 7673–7680.

111. Harrison, W.A. (2011). Origin of Sr segregation at $La_{1-x}Sr_xMnO_3$ surfaces. Phys. Rev. B *83*, 155437.

112. Chiang, Y.-M., Birnie, D.P., and Kingery, W.D. (1997). Physical Ceramics: Principles for Ceramic Science and Engineering (John Wiley & Sons, Inc.).

113. Lein, H.L., Wiik, K., and Grande, T. (2006). Kinetic demixing and decomposition of oxygen permeable membranes. Solid State Ion. *177*, 1587–1590.

114. Oh, M.-Y., Unemoto, A., Amezawa, K., and Kawada, T. (2012). Stability of $La_{0.6}Sr_{0.4}Co_{0.2}Fe_{0.8}O_{3-\delta}$ as SOFC cathode. J. Electrochem. Soc. *159*, F659–F664.

115. De Souza, R.A., Saiful Islam, M., and Ivers-Tiffée, E. (1999). Formation and migration of cation defects in the perovskite oxide $LaMnO_3$. J. Mater. Chem. *9*, 1621–1627.

116. ten Elshof, J.E., Bouwmeester, H.J.M., and Verweij, H. (1995). Oxidative coupling of methane in a mixed-conducting perovskite membrane reactor. Appl. Catal. A *130*, 195–212.

117. van Doorn, R.H.E., Bouwmeester, H.J.M., and Burggraaf, A.J. (1998). Kinetic decomposition of $La_{0.3}Sr_{0.7}CoO_{3-\delta}$ perovskite membranes during oxygen permeation. Solid State Ion. *111*, 263–272.

118. Martin, M. (2003). Materials in thermodynamic potential gradients. J. Chem. Thermodyn. *35*, 1291–1308.

119. Baumann, F.S., Fleig, J., Konuma, M., Starke, U., Habermeier, H.-U., and Maier, J. (2005). Strong performance improvement of $La_{0.6}Sr_{0.4}Co_{0.8}Fe_{0.2}O_{3-\delta}$ SOFC cathodes by electrochemical activation. J. Electrochem. Soc. *152*, A2074–A2079.

120. Wang, H., and Barnett, S.A. (2017). Sr surface segregation on $La_{0.6}Sr_{0.4}Co_{0.2}Fe_{0.8}O_{3-\delta}$ porous solid oxide fuel cell cathodes. ECS Trans. *78*, 905–913.

121. Vork, G., Chen, X., and Mims, C.A. (2005). In situ XPS studies of perovskite oxide surfaces under electrochemical polarization. J. Phys. Chem. B *109*, 2445–2454.

122. Wang, R., Zhu, Y., and Shapiro, S.M. (1998). Structural defects and the origin of the second length scale in $SrTiO_3$. Phys. Rev. Lett. *80*, 2370.

123. Bucher, E., Sitte, W., Klauser, F., and Bertel, E. (2011). Oxygen exchange kinetics of $La_{0.58}Sr_{0.4}Co_{0.2}Fe_{0.8}O_3$ at 600°C in dry and humid atmospheres. Solid State Ion. *191*, 61–67.

124. Huber, A.-K., Falk, M., Rohnke, M., Luerßen, B., Gregoratti, L., Amati, M., and Janek, J. (2012). In situ study of electrochemical activation and surface segregation of the SOFC electrode material $La_{0.75}Sr_{0.25}Cr_{0.5}Mn_{0.5}O_{3\pm\delta}$. Phys. Chem. Chem. Phys. *14*, 751–758.

125. Baharuddin, N.A., Muchtar, A., Somalu, M.R., Anwar, M., Hameed, M.A.S.A.K.A., and Mah, J. (2017). Effects of sintering temperature on the structural and electrochemical properties of $SrFe_{0.5}Ti_{0.5}O_{3-\delta}$ perovskite cathode. Int. J. Appl. Ceram. Technol. *15*, 338–348.

126. Yu, X., and Li, X. (2017). The effect of sintering temperature on the performance of IT-SOFC $SrFe_{0.9}Sb_{0.1}$ $O_{3-\delta}$ perovskite oxide. Adv. Eng. Res. *143*, 1162–1168.